Toughening Bimodal Vinyl Ester Blends Using Bio-rubber Monomers

A Thesis

Submitted to the Faculty

of

Drexel University

by

Alexander Thomas Grous

in partial fulfillment of the

requirements for the degree

of

Masters of Science in Chemical Engineering

June 2011

Dedication

Dedicated in memory of my mother, Mary Kay Grous

Acknowledgements

I would like to thank all those who have assisted me through the course of this research project at Drexel University and the U.S. Army Research Laboratory (ARL) in Aberdeen, Maryland.

I would like to specially thank my advisors, Dr. Giuseppe Palmese, Dr. Xing Geng, and Dr. John La Scala of ARL. From freshman year to the present, Dr. Palmese has always challenged me with different projects and has enlightened me on the importance of research and its real world applications. During the summer of my freshman year, Dr. Geng became my mentor, where he offered his many years of knowledge and his invaluable lab and research skills, all of which I still use today. Dr. La Scala's work set the ground work for my project and has guided me through a six month cooperative education position at ARL. The skills and knowledge that I have gained from them and through the various projects will always be much appreciated. I would also like to acknowledge the U.S. Army Research Laboratory for financial support under the Army Materials Center of Excellence Program Cooperative Agreement W911NF-06-2-0013

Thanks to the Polymer Composite Lab at Drexel, particularly Joe Stanzione, Brian Merritt, Amy Peterson, Julianne Holloway, Amutha Jeyarajasingam, Arianna Watters, James Throckmorton, and Ian McAninch. I would also like to thank the professors and staff of the department of Chemical and Biological Engineering particularly Dorothy Porter, Katie Brumbelow and Tracey McClure for all the help they have provided me.

I would like to thank my family and the Conova family for their ongoing support throughout my time at Drexel. Most importantly, I would like to thank Lauren Conova, whose patience, support, and inspiration made all of this possible.

Table of Contents

List of Tables

List of Figures

Abstract

Toughening Bimodal Vinyl Ester Blends Using Bio-rubber Monomers
Alexander Thomas Grous
Giuseppe Palmese, Ph.D.

Vinyl ester (VE) resins are commonly used as matrix materials in the manufacture of polymer matrix composites (PMC). However, most commercial VE resins are brittle and contain considerable amounts of styrene (ST) which is a hazardous air pollutant (HAP) as well as a potential carcinogen. VE resins formulated using bimodal blends of vinyl ester monomers offer both an increase in fracture performance while maintaining low viscosities without the addition of extra styrene or other additives. In this work, bio-based rubber modifiers were synthesized and combined with selected bimodal blends of VE. It was found that the addition of bio-rubbers (BR) to bimodal VE systems results in significant fracture toughness improvement by the generation of a rubbery dispersed second phase with characteristic dimensions less than 500 nm. For example, the G_{1c} of a selected VE bimodal blend initially containing 35 wt % styrene increased from 286 J/m^2 to 773 J/m^2 with the addition of 15 wt% BR. Negligible effects on the resin viscosity (~ 2300) cP were observed, the T_g remained above 100°C and styrene content was reduced to 30%. Addition of a small amount of styrene was found to reduce the viscosity of the resin to levels acceptable for liquid molding applications with minimal effects on toughness and T_g.

CHAPTER 1: INTRODUCTION

Vinyl ester (VE) resins are used for many applications in many industries including transportation, marine construction, and military. The primary use of VE is for polymer matrix composites (PMC). VE resins are a popular choice for producing PMC because of their high strength, good glass transition temperature, and their low cost. However, unmodified VE's in general have poor toughness and contain styrene (ST), which is listed in The Clean Air Act as a hazardous air pollutant (HAP) due to its toxicity and possible carcinogenicity.[1]

PMC are commonly prepared using a common, relatively inexpensive process known as Vacuum Assisted Resin Transfer Method (VARTM).[2] This is where resin is drawn into a mold and allowed to infuse into the fibers. Studies have shown that ST emissions during manufacture of PMC are a very high percentage of the total styrene emissions. This is because composite manufacturing generally mixes, infuses, and cures in open molds without any emissions controls. The Reinforced Plastic Composite National Emissions Standard for Hazardous Air Pollutants (NESHAP) went into effect in 2003 in the United States.[3] Yet, the cost of NESHAP compliance for current resin systems, processes, and cleaning techniques is high and difficult for most businesses to realize.[4] As a result, instead of using emissions controls, PMC fabricators are using low HAP VE alternatives or are switching to non-HAP epoxy resins. These low HAP alternatives include the use of a bimodal molecular weight distribution of VE monomers to decrease the amount of styrene in the system while maintaining low resin viscosities[5], or the replacement of styrene with non-volatile fatty acid monomers.[6] These efforts provide an environmentally preferred composite resin system applicable for liquid molding of military and commercial systems.

VE blends of two different molecular weight monomers can be used to obtain materials with performance characteristics of both components. Low molecular weight VE monomers have poor fracture properties due to their intrinsically high crosslink density but maintain low viscosities.[7, 8] High molecular weight VE monomers exhibit enhanced fracture properties via matrix toughening. The viscosity of the high molecular weight VE's is extremely high and requires large amounts of styrene for practical applications.[9] By mixing high molecular weight monomers with low molecular weight monomers, a low viscosity can be maintained while improving fracture properties.[10]

The second approach to modifying VE systems is the addition of modifiers to create a second dispersed phase in the vinyl ester matrix. The most frequently used modifiers are liquid rubbers based on butadiene-acrylonitrile copolymers, terminated with various functionalities like vinyl, epoxy, and carboxy. [11-16] It is believed that the rubber cavitation and subsequent shear deformation of the matrix accounts for the enhancement of fracture toughness.[17-20] However, most of these rubber modifiers are petroleum-based. Moreover, they are limited in their design and application, as a result of their limited miscibility with the VE resin.[21]

To effectively use liquid rubbers to toughen polymer resin, the rubber modifier must be miscible with the resin at processing temperature and should phase separate from solution during cure to avoid plasticizing.[12] Petroleum-based rubber modifiers typically have molecular weights of 3000-4000 g/mol and are limited in their composition. A wide range of bio-based rubber modifiers have been designed by our research group and shown to increase the properties of VE resins. These bio-based rubber modifiers use triglycerides from natural oils, such as soybean oil, as the main component of the rubber monomer. Different grafts can then be added to the triglycerides to tailor its molecular weight and functionality.[22] Geng et al. have shown that these bio rubbers (BR) were effective in increasing the G_{1c} fracture toughness of

Derakane 411-350 from ~300 J/m^2 to ~2000 J/m^2. However, when applying the same BR to monodispersed systems, the effects were less pronounced.

Due to the large use of VE in PMC and the increasing concern about the use of styrene, this work examines the properties and performance resulting from the use of BR modifiers in selected bimodal blends of VE.

CHAPTER 2: EXPERIMENTAL

Materials

Epon 828, 1001F and 1009F (Miller Stephenson), were used as the source of diglycidyl ether of bisphenol A (DEGBA). Drapex 6.8 (Chemture Corp.) was used as the source of epoxidized soybean oil for the bio rubber. Methacrylic acid (99%, Sigma Aldrich) was used to convert DGEBA to VE monomers and to methacrylate the ESO. Styrene (99%, Sigma Aldrich) was used to as reactive diluents for the VE. Octanoic acid (Sigma Aldrich), (Oct), was used to modify the methacrylated epoxidized soybean oil. AMC-2 (Aerojet Chemicals, Ranco Cordova, CA), which is a mixture of 50% trivalent organic chromium complexes and 50% phthalate esters, was used as the esterification catalyst in the addition of fatty acid chains to ESO and methacrylation of Epon and ESO. Hydroquinone (Sigma Aldrich) was used as an inhibitor for the synthesis of VE resins and the bio rubber. Trigonox 239 A (Akzo Nobel Chemicals, Chicago, Illinois), containing 45% cumene hydroperoxide, was used as the initiator for free radical polymerization of VE. Cobalt Napthenate 6% (OM Group Inc.) was used as a catalyst for Trigonox to enable room temperature curing of VE.

Vinyl Ester Preparation

VE monomers were prepared via the methacrylation of diglycidyl ether of bisphenol A (DGEBA). Epon 828, 1001F and 1009F were the source of DGEBA. Epoxy titration was performed per ASTM D1652-90, procedure B, to determine the epoxy equivalent weight of the

Epon resins.[23] The epoxy resin was dissolved in 10-15 mL of dichloromethane (SIGMA) and 10 mL of tetraethylammonium bromide solution was added. 0.1% crystal violet in acetic acid was then added to the sample and changed from blue to green when titration with perchloric acid/peracetic acid solution was complete. The epoxy equivalent weights (EEW) of the epoxy from the epoxy titration agreed well with literature values as seen in Table 1.[24]

Monodispersed VE was prepared via methacrylation of Epon 828. Approximately 300 grams of Epon 828 was reacted with 1.01 times the stoichiometic amount of methacrylic acid. 1 wt% AMC-2 was used as a catalyst for the reaction. This catalyst system is known to limit epoxy homopolymerization.[25] 0.01 wt% hydroquinone was added to prevent gelation during VE formation. The contents were added to a 1000 mL reaction vessel and briefly mixed by hand at room temperature. The vessel was then placed in a 70°C circulating temperature-controlled water bath. The contents were mechanically stirred, and temperature was monitored via OMEGA UWTC wireless thermocouples. After the initial exotherm and equilibration at 70°C, as seen in Figure 1, which occurred from 0.5-3 hours, the circulating bath was set to 90°C and the reaction was carried out to completion as determined by acid number titration. Acid number titration was used periodically to measure the unreacted acid in the system. The acid number tests were performed in accordance to ASTM-D1980-87.[26] Approximately 1 gram of VE reaction mixture was dissolved in 5 grams of acetone. Three drops of 0.5 wt% phenolphthalein in 50% ethanol indicator was added to the mixture. The solution was then titrated with 0.5 N sodium hydroxide until the solution remained pink for 30 seconds. When an acid number (mg NaOH/g VE) of less than 5 was achieved, the reaction was deemed complete. An acid number of 5 correlates to ~2% unreacted acid.

Bimodal blends of VE monomers were prepared through the methacrylation of blends of Epon 828 and either Epon 1001F or Epon 1009F. A number average molecular weight (M_n) of

800 g/mol was selected for the blended systems, as they have shown to have a high fracture toughness.[10] Epon 1001F and Epon 1009F are solids at room temperature and must be blended with Epon 828 prior to methacrylation. To aid in mixing, 20 wt% styrene was added to the Epon 828 and methacrylic acid mixture. The mixture was then placed in the circulating water bath and allowed to equilibrate at 80°C with vigorous mechanical stirring. Epon 1001F or Epon 1009F was then added in aliquots over an hour and held constant at 80°C. Once all of the high molecular weight DGEBA was dissolved in solution, the bath temperature was lowered to 70°C and 1 wt% AMC-2 and 0.01 wt% hydroquinone were added. After the initial exothermic peak equilibrated at 70°C, the system was raised to 90°C and allowed to react until an acid number of less than 5 was achieved. By controlling the temperature of the bath, external means of cooling were not required.

Gel permeation chromatography/size exclusion chromatography (GPC/SEC) was performed on all Epon and VE/ST systems to validate methacrylation of the epoxy. A Waters 515 GPC was used with two Agilient Technology PLgel-filled columns in series, each 30 cm long and 7.5 mm diameter. One column had a 50 Å pore size, and the other column had mixed pore size. The columns were equilibrated and run at 45°C using tetrahydrofuran (THF) as the elution solvent at a flow rate of 1 mL/min. The column effluent was monitored by two detectors operating at 25°C: a Waters 2410 refractive index detector and a Waters 2487 dual absorbance detector operating at 280 and 254 nm. Samples were prepared by dissolving resin samples in THF at a concentration of 1-2 mg sample/mL of THF. In GPC, the large, high molecular weight molecules cannot partition into the column packing as readily, so they elute first, while the lower molecular weight molecules diffuse into the packing and elute at higher times.[27] The Epon 828 peak occurred at 15.2 min. and the neat VE 828 peak occurred at 14.3 min. This decrease in elution time supports that methacrylation of the epoxy was successful. For the

blended systems, the VE 828 peak appeared at a slightly higher elution time but was still considered fully reacted. The difference in elution time was attributed to differences in injection timing. A large peak at 18 min was observed (not shown) that is attributed to low molecular weight species, such as styrene. There were no peaks occurring below 10 min., verifying the absence of homopolymerization.[27,28]

Mid-IR was used to measure the concentration of the unreacted epoxies and indirectly the addition of methacrylate groups. A Thermo Nicolet Nexus 870 FT-IR Spectrometer with ATR accessory was used in absorbance mode which takes 32 scans per spectrum with a resolution of 4 cm^{-1}. The epoxy peak, 912 cm^{-1}, intensity was measured at the start and end of synthesis. A decrease in intensity validated the conversion of the epoxy group to a methacrylate group. Mid IR was also used to determine the amount of styrene present in the blended VE systems after reaction. A set of VE/ST standards was made and the styrene peak intensity, 697 cm^{-1}, was recorded. The data was curve fitted so that unknown concentrations of styrene could be determined from the intensity of the styrene peak as given from the Mid IR. It was required that all neat VE systems contained 35% styrene by weight before BR was added.

Bio-rubber Preparation

The epoxy equivalent weight of ESO was determined using the same procedure as the Epon resins; ASTM D1652-90-procedure B. The molecular weight of the ESO from literature is 1000 g/mol[29] and the EEW was determined to be 248 g/mol, this verifiers the presence of 4 epoxy groups and allows for different stoichiometric ratios of methacrylic acid and fatty acids to be grafted. From previous work, it was found that a 3:1 ratio of fatty acid to methacrylic acid

performed the best.[22] Bio rubber (BR) monomers were prepared in a two step reaction. The first reaction was the methacrylation of epoxidized soybean oil. Approximately 315 grams of epoxidized soybean oil was mixed with 28 grams of methacrylic acid at room temperature. 0.5 wt% AMC-2 and 0.1 wt% hydroquinone were then added to the vessel. The contents were mixed thoroughly by hand before placing the vessel in a circulating water bath at 70°C for 1 hour. Reaction temperature was then set 90°C, and the contents reacted for approximately 3 hours.

The second stage of the reaction grafted the fatty acid molecule to the methacrylated soybean oil. The selected stoichiometric amount of fatty acid was added to the previous step's mixture. In this case, 140 grams of octanoic acid was added and reacted at 90°C for 6 hours. Acid number titration was evaluated, and the final acid number of 30 was deemed acceptable. The resulting BR molecule, Oct 3, has a calculated molecular weight of 1511 g/mol. Near IR was also conducted to ensure complete conversion of the epoxide groups.

Polymer Systems

VE/BR systems were prepared using variable amounts of a BR. Oct 3 was the BR chosen for this study because it has been shown to toughen other VE systems effectively.[22] VE 828, VE 828-1001F, and VE 828-1009F were all adjusted to contain 35wt% styrene using the Mid IR method as previously described. BR was then added to the VE systems in 5 wt% increments up to 20 wt% of the system. These systems were then mixed at room temperature for up to 5 minutes at 2000 RPM in a THINKY ARE-250 centrifugal orbital mixer. Final compositions of Vinyl

Ester/Styrene/Bio rubber (VE/ST/BR) mixtures are shown in Table 2. The addition of BR decreased the overall styrene content from 35 wt% to 28.1 wt%.

Resin Viscosity

Viscosity was measured on a TA Instruments AR 2000 ex Rhemometer in 40 mm flat plate configuration. Samples were tested at 25°C from a shear rate of 0.01 to 1000 1/s, with 10 measurements taken per decade. Shear stress was measured every 2 seconds at each shear rate and the viscosity was reported when 3 shear rate values were within 5% tolerance.

Neat Resin Cure

To effect room temperature curing of VE/ST/BR systems, 0.375 wt% CONAP was added to the mixtures and mixed at room temperature for 1 minute at 2000 RPM in a THINKY ARE-250 centrifugal orbital mixer. The initiator, Trigonox 239A, at 1.5 wt%, was then added and mixed at room temperature for 1 minute at 2000 RPM. Resins were cured at room temperature for at least 20 hours before post curing at 120°C for 2 hours.

Gel times were also studied to monitor phase separation and to observe the effects of BR on cure times. For the gel studies timing was started after the Trigonox was added to the system. Gel time was recorded when the resin could not flow from end to end in the vial when tipped.

Dynamic Mechanical Analysis

Resin bars were cast in individual silicon rubber molds with rectangular dimensions of 25 x 9 x 3 mm. Testing was carried out using a TA Instruments Q800 DMA in single cantilever geometry. Samples were tested at 1 Hz with a deflection of 15 µm and a temperature ramp from 30°C to 200°C, at a rate of 5°C/min. The temperature at which the peak in the loss modulus occurred was considered the glass transition temperature of the material.[30] To determine the glass transition temperature of the BR phase, samples were prepared and tested in the same manner, and using liquid nitrogen GCA was used to enable a -120°C to 200°C temperature range.

Miscibility of the polymer blends was determined from analysis of the storage modulus data. By taking the log of the storage modulus from room temperature to above the T_g, miscibility of the system was determined by the nature of the line as it approaches the inflection point, which occurs at the T_g of the polymer. A homogeneous single phased, (miscible) system will have a slope approaching infinity at the inflection point. An immiscible system will have a horizontal plateau where the slope of the line approaches zero. A semi-miscible system will have a constant negative slope, which is between the miscible and immiscible system.[31]

Fracture Toughness

Resin bars were cast in individual silicon rubber molds with a rectangular dimension of 0.25 x 0.5 x 3 in for use in three-point single-edge notch bend (SENB) fracture toughness. Fracture toughness was carried out in accordance to ASTM 5045-99.[32] Samples were notched in

the center using a diamond saw. Then, a razor blade was used to initiate a crack at the base of the notch. The samples were tested on an INSTRON 8872 with a 1 kN load cell in flexural mode with a cross head rate of 10 mm/min. All samples were tested at ambient conditions. Calculation of the G_{1c} was done in accordance with the ASTM standard, using the correction displacement method. Further description of correction displacement method is given in APPENDIX E: Explanation of Correction Displacement Method.

Surface Morphology

Surface morphology of the fractured surfaces was observed using scanning electron microscopy (SEM). For comparison, evaluation was conducted on samples prepared via liquid nitrogen fracture and on the broken surfaces of fracture toughness samples. SEM was performed using a ZEISS Supra 50VP in Backscatter SE2 and Inlens arrangements.

Table 1: Epoxy equivalent weights as determined by epoxy titration and literature values as well as the calculated molecular weights for the epoxy and VE monomers.

Epon Resin	Literature EEQ (g/mol)	Experimental EEQ (g/mol)	Calculated MW (g/mol)	Calculated VE Mw (g/mol)
828	185-192	188	377	549
1001F	525-550	536	1072	1344
1009F	2300-3800	2826	5651	5823

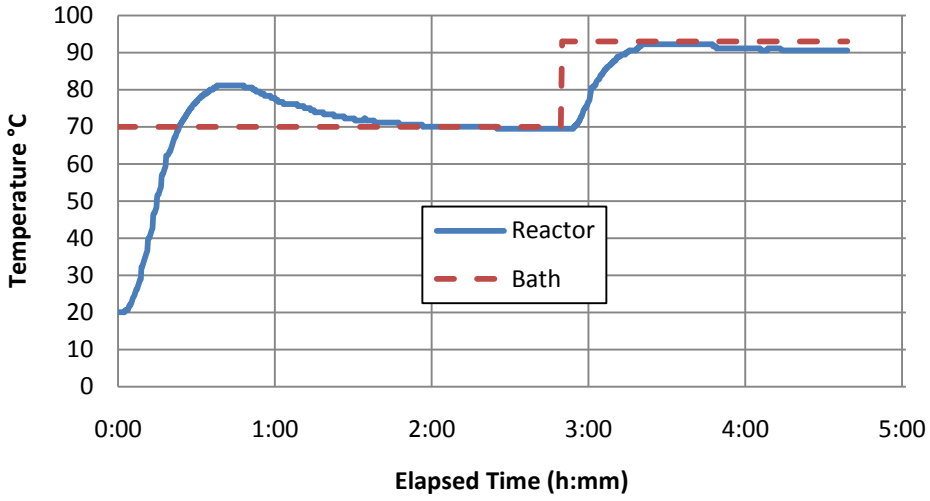

Figure 1: Temperature profile during VE synthesis.

Table 2: Experimental ratios of VE/ST/BR used throughout this work where X denotes either 828, 828-1001F or 828-1009F.

Sample ID	Wt% VE	Wt% Styrene	Wt% Oct 3
VE-X 0% BR	65.00%	35.00%	0.00%
VE-X 5% BR	61.75%	33.25%	5.00%
VE-X 10% BR	58.50%	31.50%	10.00%
VE-X 15% BR	55.25%	29.75%	15.00%
VE-X 20% BR	51.90%	28.10%	20.00%

CHAPTER 3: RESULTS AND DISCUSSION

Viscosity

As seen in Table 3, the viscosities of the resins show that viscosity is dependent on both the blend type and the amount of BR in the system. VE 828, with a molecular weight of 549.0 g/mol, has a viscosity of 76 cP. The VE blends, VE 828-1001F and VE 828-1009F, have viscosities of 816 cP and 2133 cP, respectively. Since both resins were synthesized with the same number average molecular weight, individual components still contribute to the overall viscosity of the blend.

The viscosity of Oct 3 was found to be 2464 cP. For all three systems, VE 828, VE 828-1001F and VE 828-1009F, the addition of BR increased the viscosity. For VE 828, the addition of 20% Oct 3 doubled the viscosity of the system, while for the VE 828-1001F system, a 20% addition of Oct 3 increased the viscosity by about 200 cP. For the VE 828-1009F system, the addition of BR had a negligible effect on the viscosity of the system.

For VARTM purposes, a rule of thumb is that a resin viscosity of about 500 cP is desirable.[33] To create a VE/BR system that meets this standard, styrene was added in 5% increments to the VE 828-1009F 15% Oct 3 system. A viscosity of 463.46 cP was achieved at 40 wt% styrene in the VE 828-1009F Oct system. Achieving a viscosity of less than 500 cP with only 40 wt% styrene in a toughened system is significant because typically, additives increase the viscosity greatly and make the resin unsuitable for VARTM processes unless significantly greater amounts of styrene are added.

Processability

VE resins used in transfer molding must exhibit certain properties, such as uniform phase, low viscosity, and sufficient working times. In phase separating systems, controlling when phase separation occurs is important. Systems that are initially uniform and settle over time are not process favorable and lengthen production periods. When first synthesized, the bimodal blends contained less than 20 wt% styrene and separation of the two blends was observed after 6 months at rest, as seen Figure 2. However, at 35 wt% styrene, phase separation of VE monomers was not observed. For VE 828 and VE 828-1001F, BR was loaded up to 20% and did not exhibit any liquid phase separation for up to 9 months. For the VE 828-1009F system, the 20wt% BR phase separated almost immediately after mixing, as seen in Figure 3. For VE 828-1009F, loading up to 15 wt% BR did not exhibit liquid phase separation for up to 9 months.

As discussed earlier, viscosity is important for the processability of the resin, because if the resin is too viscous, incomplete infusion and or incomplete fiber wetting may occur. Gel time can also affect the processability of the resin because too short of gel times can also result in incomplete infusion of the part. For large parts, it is important for the resin to fully impregnate the part, so long working times are desirable. However, extensive working times can impede productivity. When using resin transfer molding techniques, gel times can be tailored using various cure packages. In phase separating systems, extended cure times by altering the cure package did not affect the overall mechanical properties of the system. However, lower T_g's were observed due to the plasticizing additive resulting from the cure package.

As seen Table 4, by using a standard cure package, a proportional relationship of increasing gel times and increasing amount of BR was observed. The amount of styrene had little effect on the gel times, as increasing the system from 30% to 40% resulted in only a change of 5 minutes. The gel times from one VE system to another increased. This is probably due to the high concentration of hydroquinone inhibitor used in the synthesis of BR.

In most systems, visually observable phase separation began after gelation. However, the occurrence of phase separation before gelation was noticed in VE 828-1001F 20% Oct 3 and for all VE 828-1009F with more than 10% Oct 3. The degree of phase separation also varied with time. Once the systems were gelled, phase separation continued for an additional 2 hours. The evolution of phase separation observed by increasing opacity of samples with time is shown in Figure 4 for a representative system comprised of VE 828-1009F Oct 3 with 40% styrene.

To monitor phase separation, a glass slide was surrounded with tacky tape to create a well of approximate dimensions of 60 x 20 x 3 mm. Photographs were taken to track the extent of phase separation. The initial phase separation was observed at 64 minutes prior to the gelation (95 minutes) and continued after gelation for a considerable period of time. It is expected that the sizes of the particles are controlled also by constraining effects of crosslinked polymer matrix. The increasing opacity could also be a result of the changing index of refraction with extent of conversion.

Dynamic Mechanical Analysis

Figure 5 shows the storage and loss modulus for the 35 wt% styrene neat VE's as a function of temperature. The presence of one sharp loss modulus peak indicates that the VE

828-1001F and VE 828-1009F blends were miscible. The glass transition temperature of the blended systems, VE 828-1001F and VE 828-1009, were both around 122°C. The blended systems both had lower glass transition temperature compared to that of the mondisperse VE 828 system, which had a T_g of 138°C. This decrease in glass transition temperature is expected, as the T_g of the higher molecular weight VE ester systems is substantially lower.

Glass transition temperature was also affected by the amount of BR added to the system, as seen in Table 5. For VE 828, the addition Oct 3 caused T_g to decrease from 138°C with no Oct 3 to 106°C with 20 wt% Oct 3. The change in T_g with BR loading was greatest at low concentration. For the VE 828-1001F blend, the pattern was similar to the VE 828 system. The T_g of the neat VE 828-1001F system was 122°C and deceased to 94°C with 20 wt% Oct 3. The T_g of the VE 828-1009F blends also decreased with the addition of BR. However, very little change in T_g was observed between 10 wt% and 15 wt% BR. Overall all systems experience the greatest decrease in Tg with BR loading at low concentration suggesting that a portion of the BR remains dissolved in the matrix reducing the Tg by plasticization.

In general, the decline in T_g was followed with a widening of the loss modulus peak. This widening indicates the existence of an inhomogeneous network. For VE-828 and VE 828-1001F systems, phase separation was observed in conjunction with significant broadening of the loss modulus peak at 5 wt% loading of BR or greater. For VE 828-1009F, loading of up to 15 wt% BR was achieved without significant widening of the loss modulus peak. This suggests that a more uniform phase separation occurs in this system.

Styrene content had minimal effect of T_g in the VE 828-1009F system, as no significant change in T_g was observed (Table 5). With the hope of determining the T_g of the phase separated BR, samples of VE/BR/ST DMA traces were obtained from -120°C to 200°C. The T_g of the BR is expected to be lower than room temperature due to the chemical structure. All

polymer systems exhibited a β-relaxation between -79°C to -87°C. In most systems, no additional peaks were noticeable between the β-relaxation peak and the T_g. However, all systems having higher BR content investigated showed a third peak. In the VE 828 system with 20% loading of BR, an additional peak at -36.1°C was observed as seen in Figure 6. For the blended systems, the additional peak occurred at a higher temperature than in the VE 828 system. For VE 828-1001F with 20% loading of BR, the peak occurred at -26.1°C, while the peak occurred at -28.9°C in the VE 828-1009F system with 15% BR content. These T_g values are thought to represent the T_g of the dispersed rubber phase. Generally DMA can capture the behavior of second phase particles if they have dimension on the order of 1 μm or more. The absence of a specific transition for the systems with lower BR content does not necessarily mean a second phase does not exist. In fact one with characteristics dimensions less than a few hundred nanometers would not be apparent.

When the upper limit of BR loading evaluated was not dictated by the liquid phase behavior, analysis of the storage modulus as described in the experimental section was done (Figure 7). The VE 828 neat resin showed a sharp inflection point, indicating a fully miscible system, which is expected. The miscibility of the VE 828-1001F and VE 828-1009F blends were determined to be fully miscible because the nature of the lines match closely with the VE 828 system. The VE 828 BR series displayed semi-miscible nature at higher loading of BR, as displayed by flattening of the slope. In both VE blends, miscibility was maintained even at high BR loading. At no point did the systems become fully immiscible.

Fracture Toughness

For unmodified systems the fracture toughness was found to increase as the number average molecular weight of vinyl esters increased. This increase in fracture toughness was caused by matrix toughening.[7] As seen in Table 6, the G_{1C} of the low molecular weight resin system, VE 828, was determined to be 190±44 J/m^2. This value is significantly higher than values as reported by La Scala et al., who reported values of 85-110 J/m.[2,5] This increase is attributed to variations in sample preparation with methods of crack initiation. For the higher molecular weight blends, the fracture toughness was comparable. G_{1C} values of 272±50 J/m^2 for the VE 828-1001F system and a G_{1C} value of 286±48 J/m^2 for the VE 828-1009F system were measured. These values are similar with previous values as reported by La Scala et al. and are comparable to values for 411-350, which is a commercial VE containing 45 wt% styrene.

VE 828-1009F was chosen to evaluate the full effect of BR on fracture toughness. For the VE 828 and VE 828-1001F systems, the maximum loading was 5% BR. For all systems, the increase in BR resulted in an increase in fracture toughness. In VE 828-1009F, the fracture toughness continued to increase up to 15% BR loading. The increase in fracture toughness from 0% to 5% BR and from 5% to 10% BR almost doubled the value of G_{1C}. However, from 10% to 15% BR, fracture toughness only increased by about 40 J/m^2. This indicates that there is a maximum loading threshold of BR in VE systems. Loading above this threshold does not appear to significantly affect the fracture toughness of the system.

In the VE 828-1009F Oct 3 40% styrene system, the G_{1C} was 543±107 J/m^2. This value was lower than expected because the BR content is 12.8%. However, the styrene content was

significantly higher than the other systems at 40.0 wt%. High styrene concentrations are known to create polystyrene zones which are brittle and reduce the fracture properties.[34]

Surface Morphology

The fracture surface of the neat resins and the toughened VE systems were examined by SEM. As seen in Figure 8, the surface of the neat resins as prepared by liquid nitrogen fracture differed from system to system. The VE 828 fracture surface was smoother than the surface of the VE 828-1009F system, as the VE 828-1009F system exhibited a very rough surface. The increased surface roughness was expected as the fracture toughness for VE 828-1009F was almost twice that of the VE 828 system.

The neat VE 828-1009F resin and the VE 828-1009F resin with 15 Oct 3 fracture toughness samples' facture surfaces show very different fracture surface morphologies, as seen in Figure 9. The neat resin has a smooth uniform surface, while the BR modified system has much more depth and the appearance of small, circular voids. The uniformly dispersed second phase consists of domains less than 500 nm in diameter. Their counterpart, the void, appears to be asymmetric and suggests the occurrence of cavitation. This suggests that significant matrix shear deformation occurs, which would explain the high fracture toughness values that were obtained.

Voids were not as clearly discernible in the VE 828-1009F 5 wt% Oct systems, as seen in Figure 10. A close look shows the existence of voids less than 100 nm. Yet, there was a significant increase in fracture toughness from the base resin. The voids and particles were also smaller in the VE 828-1009F 10 wt% Oct 3 system than the VE 828-1009F 15 wt% Oct 3,

perhaps being about 200 nm. Despite having a smaller size and overall lower concentration, the G_{1c} of VE 828-1009F 10 wt% Oct was found to be almost had the same as that of the VE 828-1009F 15 wt% Oct 3 system. This suggests that there is an optimal particle size where fracture toughness is maximized.

Additional SEM micrographs for all samples can be found in APPENDIX G: Additional SEM Micrographs.

Table 3: The viscosities for VE/ST/BR systems showing a proportional increase in viscosity and BR.

Sample Name	Wt% Oct 3	Wt% Styrene	Viscosity (cP)
VE 828 0% Oct 3	0.00	34.9	76
VE 828 5% Oct 3	5.03	33.1	102
VE 828 10% Oct 3	10.02	31.4	128
VE 828 15% Oct 3	15.01	29.6	138
VE 828 20% Oct 3	19.98	28.0	167
VE 828-1001F 0% Oct 3	0.00	36.1	816
VE 828-1001F 5% Oct 3	5.02	34.3	900
VE 828-1001F 10% Oct	10.00	32.5	869
VE 828-1001F 15% Oct 3	15.29	30.6	1001
VE 828-1001F 20% Oct 3	20.02	28.9	1019
VE 828-1009F 0% Oct 3	0.00	35.0	2133
VE 828-1009F 5% Oct 3	5.01	33.3	2200
VE 828-1009F 10% Oct 3	10.03	31.5	2182
VE 828-1009F 15% Oct 3	15.02	29.7	2272
VE 828-1009F Oct 3 29.75% ST	15.00	29.8	2301
VE 828-1009F Oct 3 30% ST	14.95	30.0	2205
VE 828-1009F Oct 3 35% ST	13.88	35.0	977
VE 828-1009F Oct 3 40% ST	12.81	40.0	464

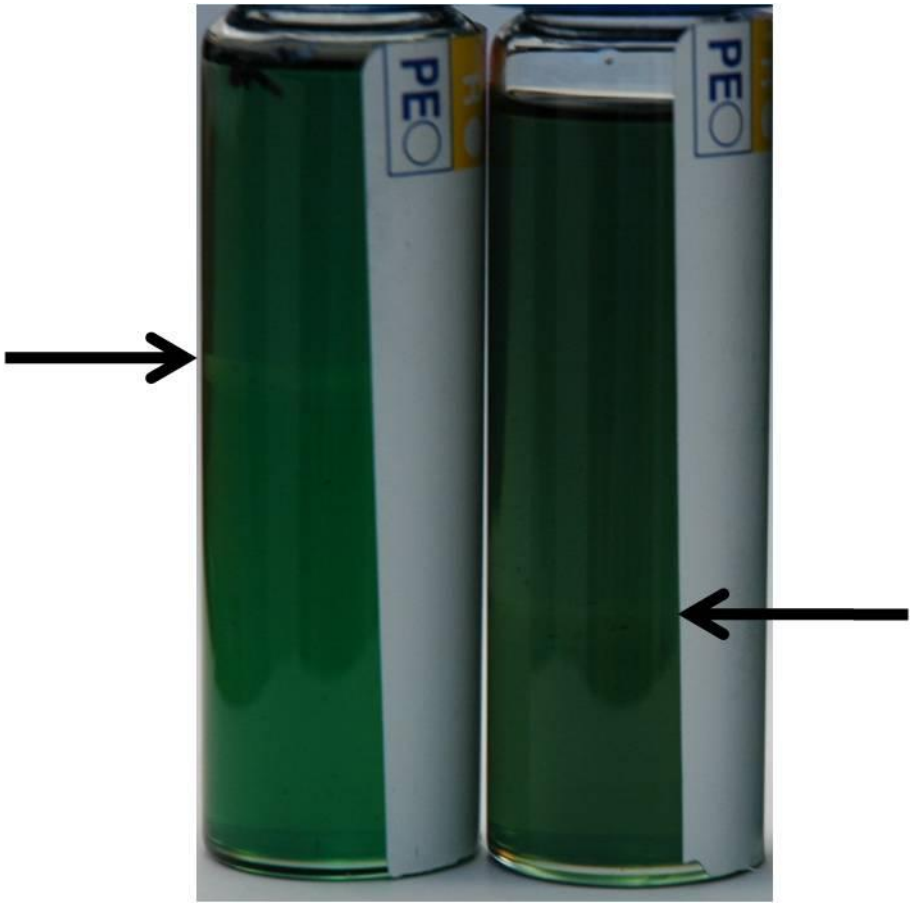

Figure 2: Bimodal blend separation of low styrene content VE 828-1001F (left) and VE 828-1009F (right).

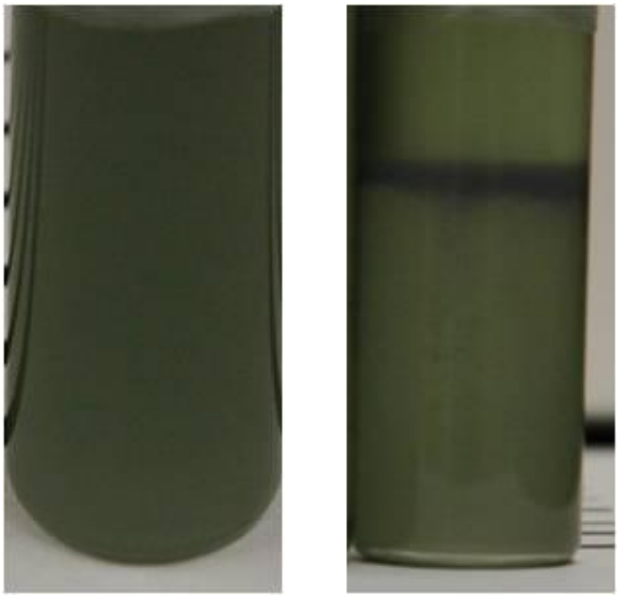

Figure 3: VE 828-1009F 20% BR phase separation after mixing (left) and after 24 hours (right).

Table 4: Gel times for VE/BR/ST systems.

Sample Name	Gel Time [min:ss]
VE 828 0% Oct 3	6:04
VE 828 5% Oct 3	10:15
VE 828 10% Oct 3	17:10
VE 828 15% Oct 3	36:30
VE 828 20% Oct 3	45:44
VE 828-1001F 0% Oct 3	14:31
VE 828-1001F 5% Oct 3	15:55
VE 828-1001F 10% Oct	22:03
VE 828-1001F 15% Oct 3	36:07
VE 828-1001F 20% Oct 3	62:14
VE 828-1009F 0% Oct 3	28:00
VE 828-1009F 5% Oct 3	30:23
VE 828-1009F 10% Oct 3	35:25
VE 828-1009F 15% Oct 3	81:44
VE 828-1009F Oct 3 30% ST	79:49
VE 828-1009F Oct 3 35% ST	82:27
VE 828-1009F Oct 3 40% ST	84:00

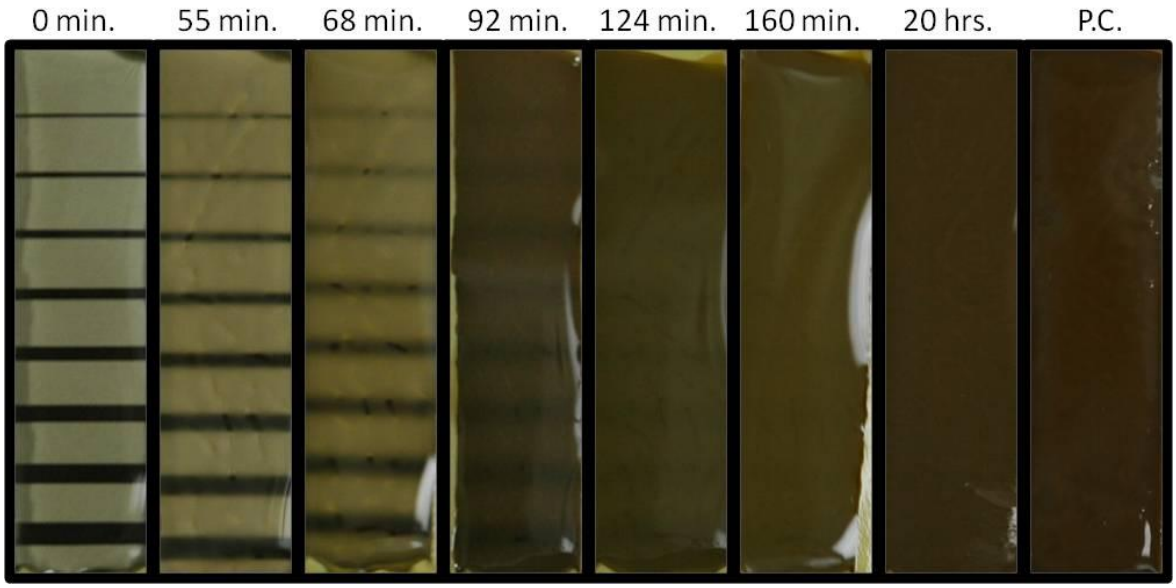

Figure 4: Phase separation increases with time as the VE 828-1009F Oct 3 40% styrene polymer network cures.

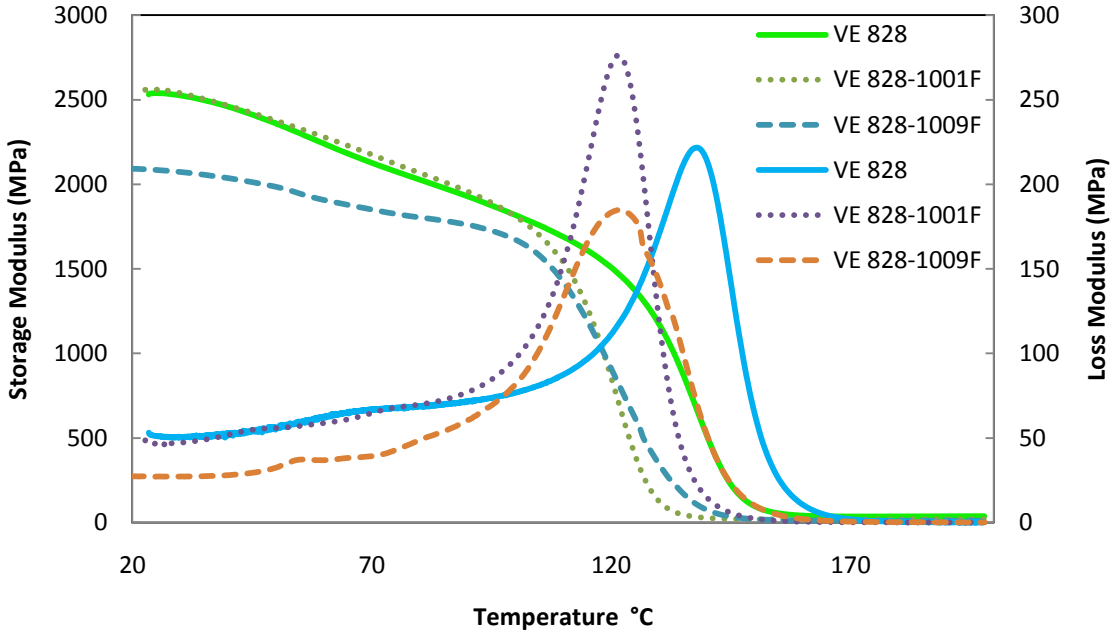

Figure 5: Dynamic Mechanical properties showing the storage modulus (decreasing) and the loss modulus (maximum) of 35 wt% styrenated batch VE's.

Table 5: Glass transition and beta transition temperatures of the polymer systems.

Sample Name	T_g °C	β-peak °C
VE 828 0% Oct 3	138	-87
VE 828 5% Oct 3	126	-85
VE 828 10% Oct 3	115	-85
VE 828 15% Oct 3	112	-84
VE 828 20% Oct 3	106	-82
VE 828-1001F 0% Oct 3	122	-86
VE 828-1001F 5% Oct 3	105	-85
VE 828-1001F 10% Oct	100	-84
VE 828-1001F 15% Oct 3	96	-84
VE 828-1001F 20% Oct 3	94	-81
VE 828-1009F 0% Oct 3	122	-79
VE 828-1009F 5% Oct 3	107	-83
VE 828-1009F 10% Oct 3	102	-79
VE 828-1009F 15% Oct 3	103	-79
VE 828-1009F Oct 3 30% ST	100	-
VE 828-1009F Oct 3 35% ST	102	-
VE 828-1009F Oct 3 40% ST	101	-

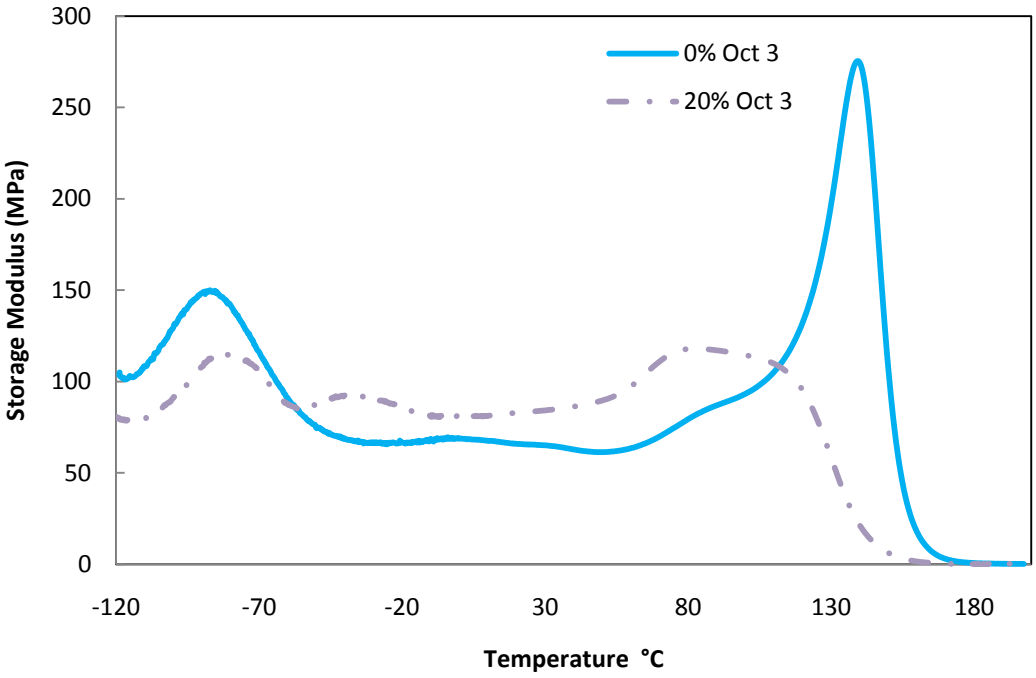

Figure 6: Low temperature DMA of VE 828 20% Oct 3. The evolution of the peak occurring below -20 ° C was taken to be the T_g of the BR.

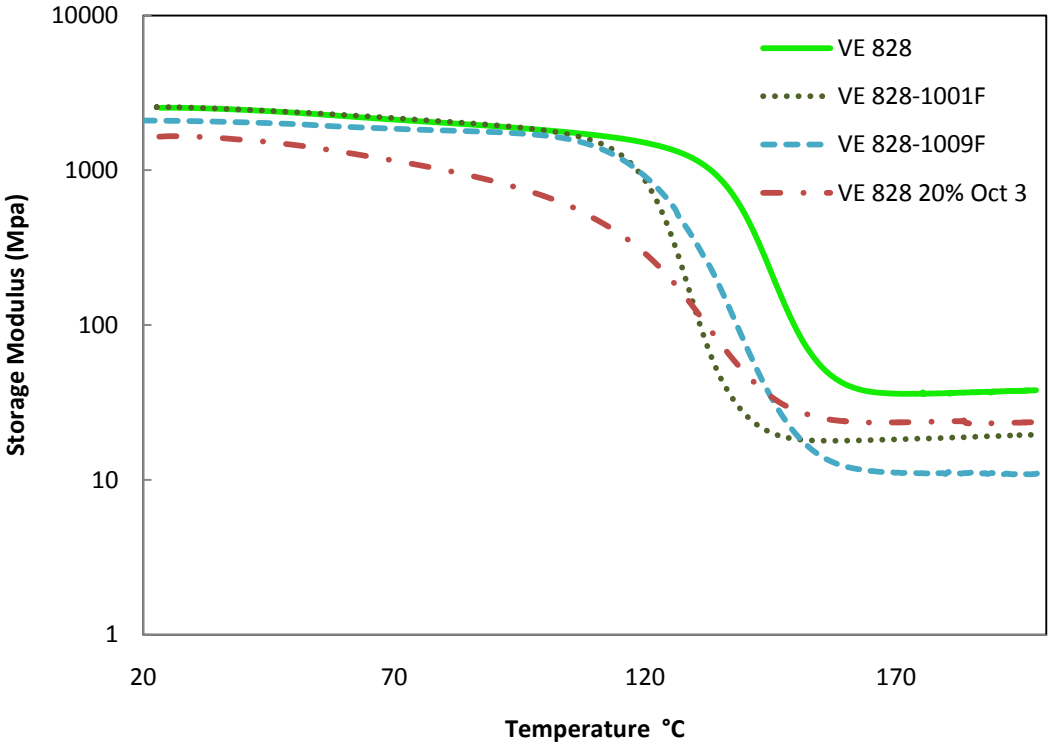

Figure 7: The miscibility of cured VE 828-BR series can be determined by viewing the storage modulus on a log scale versus temperature. As miscibility decreases, the slope of the line decreases as observed at 20% BR loading.

Table 6: Fracture toughness values for VE/ST/BR systems.

Sample Name	K_{1C} (Mpa-$m^{1/2}$)	G_{1C} (J/m^2)
VE 828 0% Oct 3	0.83±0.11	190±44
VE 828 5% Oct 3	0.86±0.08	233±68
VE 828-1001F 0% Oct 3	0.98±0.09	272±50
VE 828-1001F 5% Oct 3	1.05±0.1	355±126
VE 828-1009F 0% Oct 3	1.04±0.05	286±48
VE 828-1009F 5% Oct 3	1.22±0.17	406±148
VE 828-1009F 10% Oct 3	1.74±0.17	736±114
VE 828-1009F 15% Oct 3	1.68±0.17	781±175
VE 828-1009F Oct 3 40% ST	1.17±0.16	543±107
Derakane 411-350[22]	-	255±55

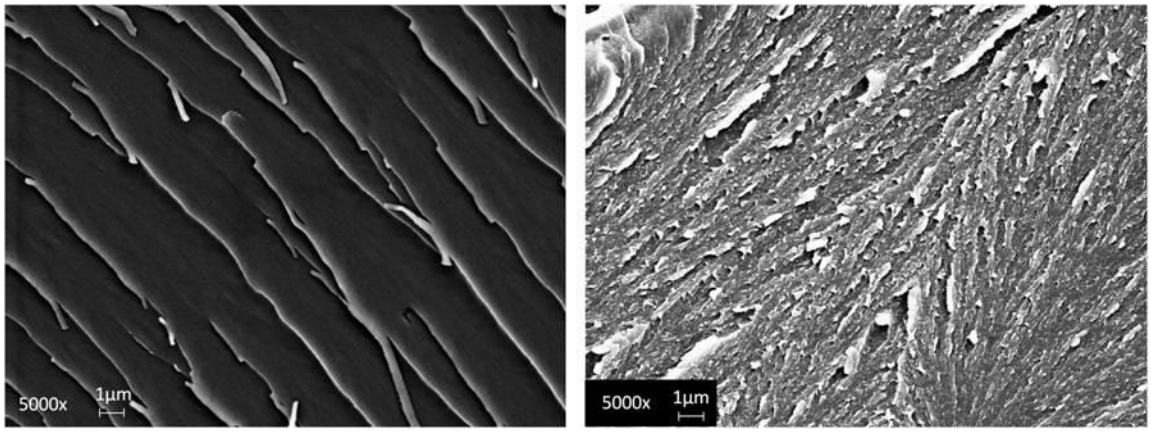

Figure 8: Neat resin surface morphology of liquid nitrogen prepared VE 828 (left) and VE 828-1009F (right).

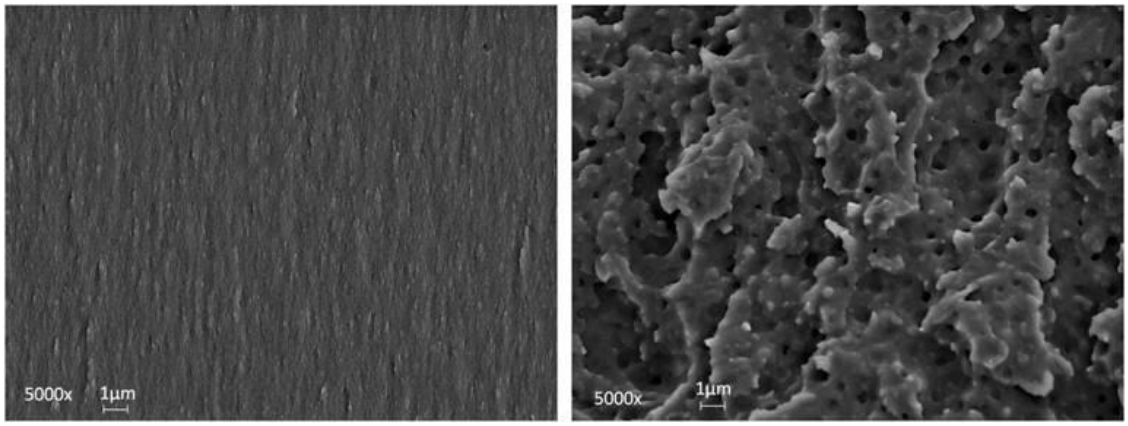

Figure 9: SEM micrographs of the neat VE 828-1009F resin (left) and the VE 828-1009F resin with 15% Oct 3 (right).

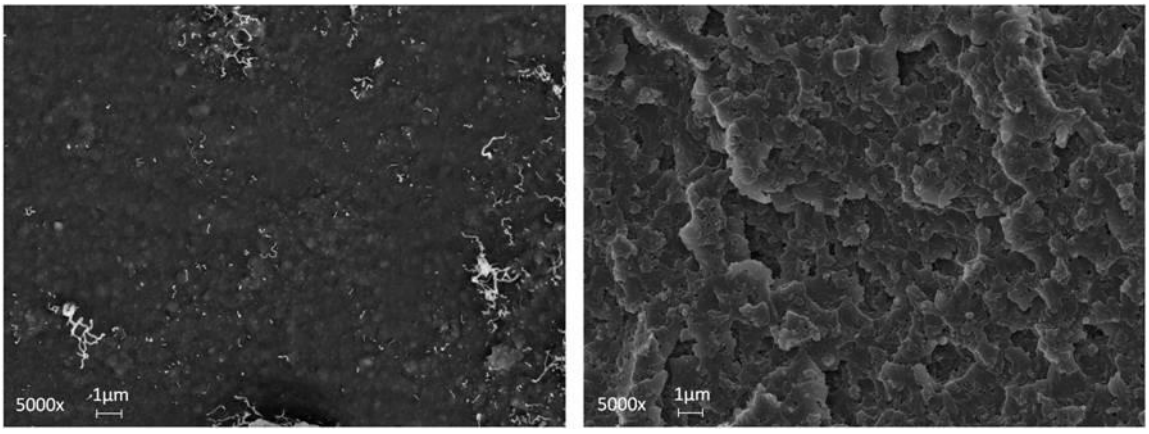

Figure 10: SEM micrographs of the VE 828-1009F resin modified with 5 wt% Oct 3 (left) and 10 wt% Oct 3 (right).

CHAPTER 4: CONCLUSIONS

In this work, bio-based rubber modifiers were synthesized and combined with selected bimodal blends of VE. It was found that the addition of bio-rubbers (BR) to bimodal VE systems results in significant fracture toughness improvement by the generation of a rubbery dispersed second phase with characteristic dimensions less than 500 nm. For example, the G_{1c} of a selected VE bimodal blend containing 35 wt % styrene increased from 286 J/m^2 to 773 J/m^2 with the addition of 15 wt% BR. Negligible effects on the resin viscosity (~ 2300) cP were observed, the T_g remained above 100°C and styrene content was reduced to 30%. Addition of a small amount of styrene was found to reduce the viscosity of the resin to levels acceptable for liquid molding applications with minimal effects on toughness and T_g.

Recommendations

The characterization of BR in bimodal blends was limited because only one BR and one number average molecular weight VE were chosen for the investigation. Because of the poor performance of the particular BR in the monodispersed system and the good performance exhibited in the blends, different molecular weight BR's may have different behavior when combined with vinyl ester systems having other molecular weights. If it is found that different molecular weight BR's can be more effective in low molecular weight monodispersed systems, distributed molecular weight BR blends may prove useful for obtaining improved blended VE systems.

List of References

1. Bassett, S. (Ed.). (2003). *Emission Control Strategies: A Guide for Composites Manufacturers*. Wheat Ridge, CO: Ray Publishing, Inc.

2. Campbell, F. C. (2004). *Manufacturing processes for advanced composites*: Elsevier Science.

3. Agency, E. P. (2003). *National emissions standard for hazardous air pollutants: reinforced plastic composites productions.*: Federal Register.

4. Vallone, J. (2004). NESHAP Requirements Assessment for Miscellaneous Coatings, Adhesives, Sealers, Etc. *Final Report to ARL, Sustainable Painting Operations for the Total Army*.

5. La Scala, J. J., Logan, M. S., Sands, J. M., & Palmese, G. R. (2008). Composites based on bimodal vinyl ester resins with low hazardous air pollutant contents. *Composites Science and Technology, 68*(7-8), 1869-1876.

6. La Scala, J. J., Sands, J. M., Orlicki, J. A., Robinette, E. J., & Palmese, G. R. (2004). Fatty acid-based monomers as styrene replacements for liquid molding resins. *Polymer, 45*(22), 7729-7737.

7. Huang, Y., Hunston, D., Kinloch, A. J., & Riew, C. K. (1993). Mechanisms of toughening thermoset resins. *Advances in chemistry series, 233*, 1-1.

8. LeMay, J., & Kelley, F. (1986). Structure and ultimate properties of epoxy resins. In K. Dušek (Ed.), *Epoxy Resins and Composites III* (Vol. 78, pp. 115-148): Springer Berlin / Heidelberg.

9. Products, R. P. (2001). *Physical Properties Guide for Epoxy Resins and Related Products*. Houston.

10. La Scala, J. J., Orlicki, J. A., Winston, C., Robinette, E. J., Sands, J. M., & Palmese, G. R. (2005). The use of bimodal blends of vinyl ester monomers to improve resin processing and toughen polymer properties. *Polymer, 46*(9), 2908-2921.

11. Auad, M. L., Frontini, P. M., Borrajo, J., & Aranguren, M. I. (2001). Liquid rubber modified vinyl ester resins: fracture and mechanical behavior. *Polymer, 42*(8), 3723-3730.

12. Robinette, E., Ziaee, S., & Palmese, G. (2004). Toughening of vinyl ester resin using butadiene-acrylonitrile rubber modifiers. *Polymer, 45*(18), 6143-6154.

13. Dreerman, E., Narkis, M., Siegmann, A., Joseph, R., Dodiuk, H., & Dibenedetto, A. (1999). Mechanical behavior and structure of rubber modified vinyl ester resins. *Journal of Applied Polymer Science, 72*(5), 647-657.

14. Ullett, J. S., & Chartoff, R. P. (1995). Toughening of unsaturated polyester and vinyl ester resins with liquid rubbers. *Polymer Engineering & Science, 35*(13), 1086-1097.

15. Stevanovic, D., Lowe, A., Kalyanasundaram, S., Jar, P. Y. B., & Otieno-Alego, V. (2002). Chemical and mechanical properties of vinyl-ester/ABS blends. *Polymer, 43*(16), 4503-4514.

16. Pham, S., & Burchill, P. (1995). Toughening of vinyl ester resins with modified polybutadienes. *Polymer, 36*(17), 3279-3285.

17. Bascom, W., Cottington, R., Jones, R., & Peyser, P. (1975). The fracture of epoxy and elastomer modified epoxy polymers in bulk and as adhesives. *Journal of Applied Polymer Science, 19*(9), 2545-2562.

18. Bascom, W., Ting, R., Moulton, R., Riew, C., & Siebert, A. (1981). The fracture of an epoxy polymer containing elastomeric modifiers. *Journal of materials science, 16*(10), 2657-2664.

19. Pearson, R. A., & Yee, A. F. (1986). Toughening mechanisms in elastomer-modified epoxies. *Journal of materials science, 21*(7), 2475-2488.

20. Yee, A. F., & Pearson, R. A. (1986). Toughening mechanisms in elastomer-modified epoxies. *Journal of materials science, 21*(7), 2462-2474.

21. Doi, M. (1996). *Introduction to polymer physics*: Oxford University Press, USA.

22. Geng, X. (2010). *Design of Epoxidized Soybean Oil Based Bio-rubber for Vinyl Ester and Unsaturated Polyester Resin Toughening*. Philadelphia: Drexel University Department of Chemical Engineering.

23. International, A. (1990). ASTM D 1652-90, *Standard Test Methods for Epoxy Content of Epoxy Resins* (pp. 341-343). West Conshohocken, PA.

24. Chemicals, H. S. (2009). *EPON and EPI-REZ Epoxy Resins Product Overview*. Columbus, OH.

25. Aerojet. (2000). Product Bulletin for Aerojet Accelerator, AMC-2. In A. Chemicals (Ed.). Rancho Cordova, CA.

26. International, A. (1987). ASTM D 1980-87, *Standard Test Method for Acid Value of Fatty Acids and Polymerized Fatty Acids* (pp. 428-429). West Conshohocken, PA.

27. Garcia, A. A. (1999). *Bioseparation process science*: Wiley.

28. Khot, S. N. (2001). *Synthesis and application of triglyceride based polymers.* University of Delaware.

29. Chemtura. (2007). Drapex 6.8 Epoxidized Soybean Oil. In C. Corporation (Ed.) (pp. 1-6). Middlebury, CT.

30. Nielsen, L. E., & Landel, R. F. (1994). *Mechanical properties of polymers and composites*: CRC Press.

31. Sperling, L. H. (1992). *Introduction to physical polymer science*: Wiley Online Library.

32. International, A. (1999). ASTM D 5045-99, *Standard Test Methods for Plane-Strain Fracture Toughness and Strain Energy Release Rate of Plastic Materials* (pp. 1-9). West Conshohocken, PA.

33. Kulshreshtha, A. K., & Vasile, C. (2003). *Handbook of polymer blends and composites*: iSmithers Rapra Publishing.

34. Ziaee, S., & Palmese, G. R. (1999). Effects of temperature on cure kinetics and mechanical properties of vinyl–ester resins. *Journal of Polymer Science Part B: Polymer Physics, 37*(7), 725-744.

APPENDIX A: Pictures of Reactor Vessel

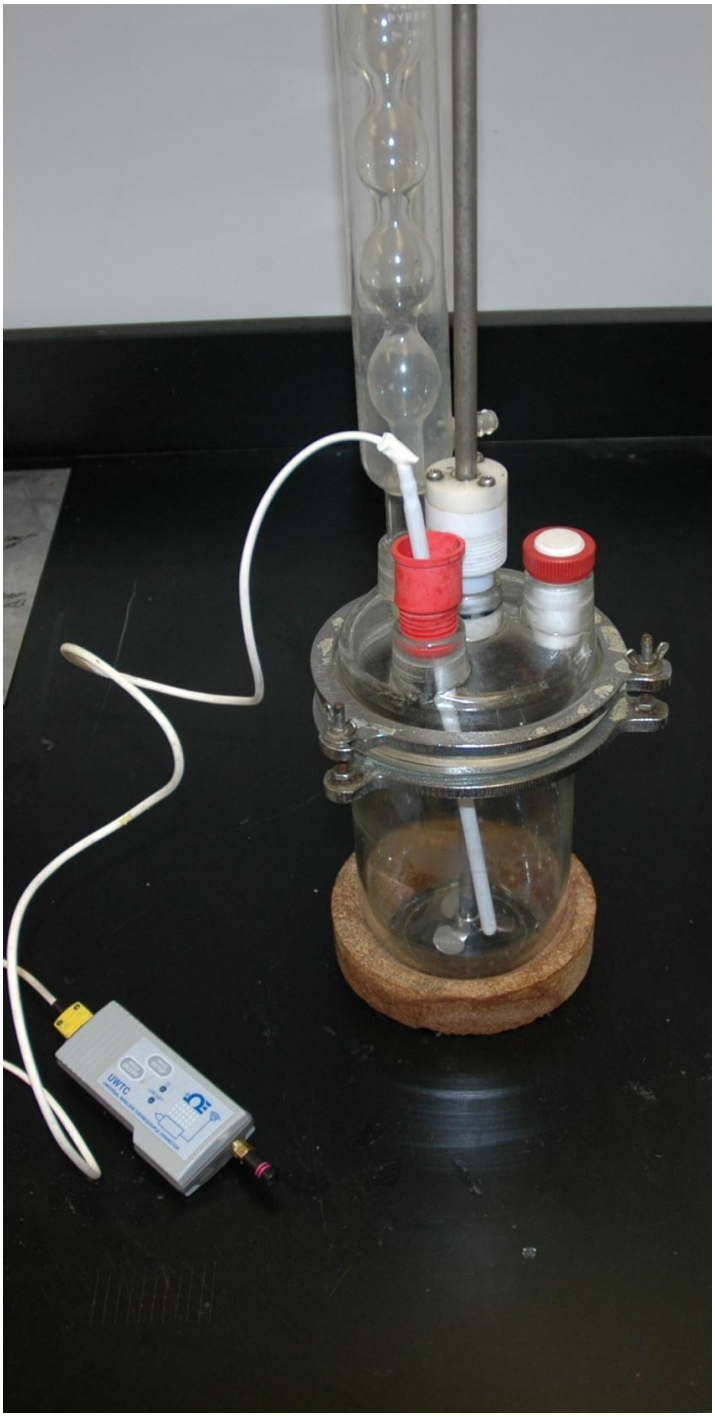

Figure 11: 1000 mL reaction vessel with wireless thermocouple, condensation tube and stirrer.

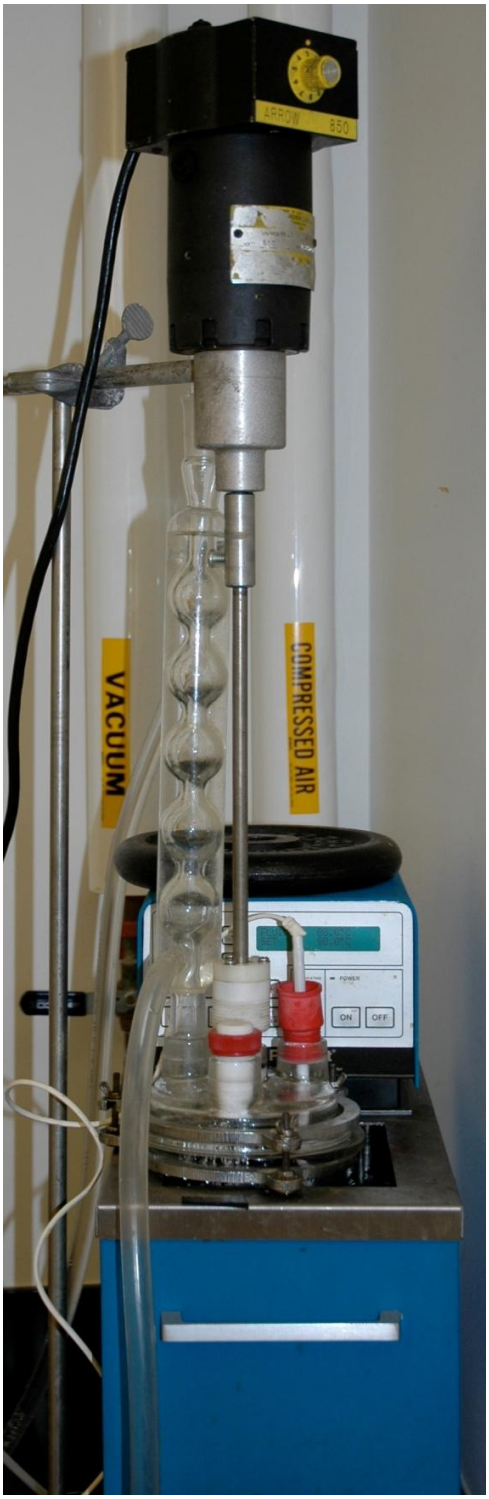

Figure 12: Reaction vessel in circulating water bath unit with mechanical stirrer.

APPENDIX B: Additional Processability Pictures

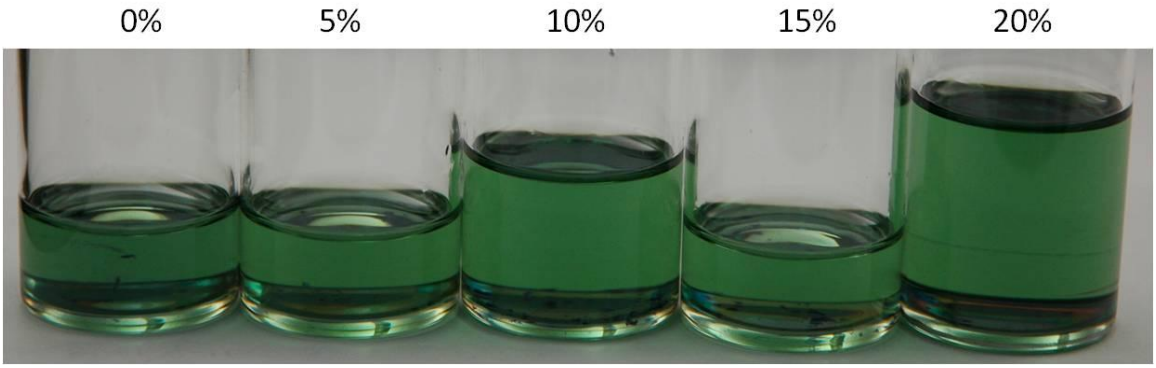

Figure 13: VE 828 with varied loadings of BR after 9 months of inactivity.

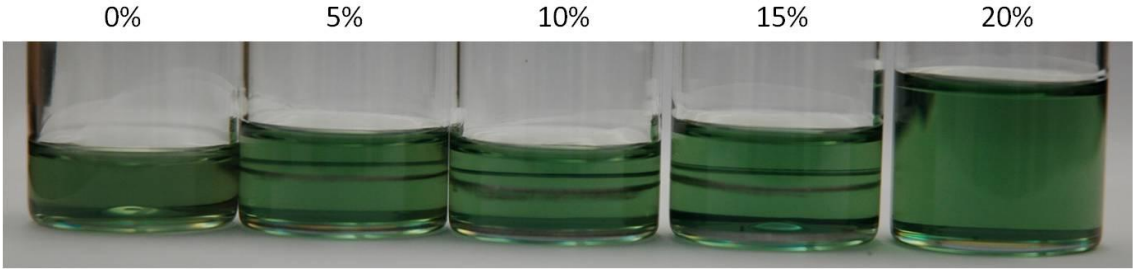

Figure 14: VE 828-1001F with varied loadings of BR after 9 months of inactivity. Note the rings observed in samples 5-15 wt% BR are on the outside of vial.

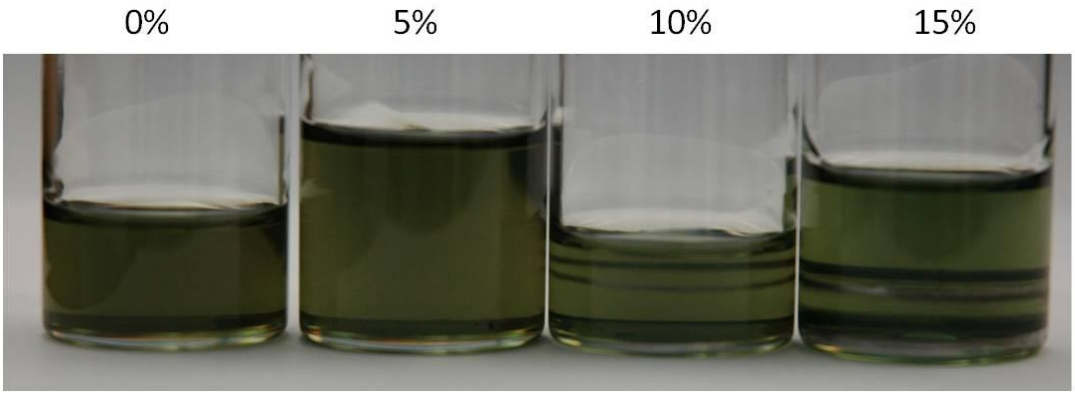

Figure 15: VE 828-1009F with varied loadings of BR after 9 month of inactivity. Note the rings observed in samples 10 and 15 wt% BR are on the outside of vial.

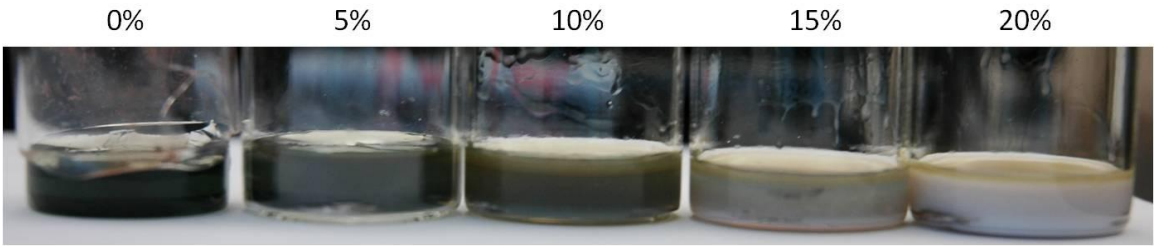

Figure 16: Room temperature cured VE 828 with varied BR content.

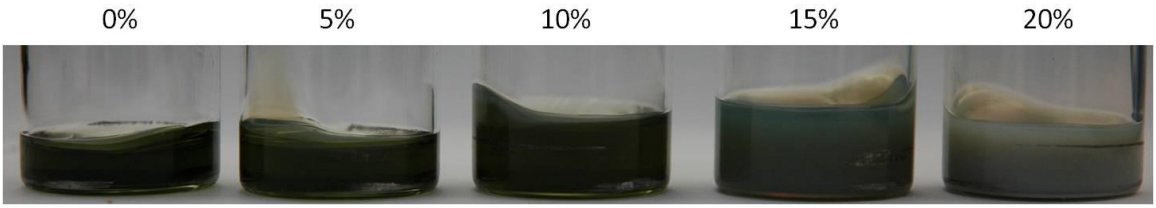

Figure 17: Room temperature cured VE 828-1001F with varied BR content.

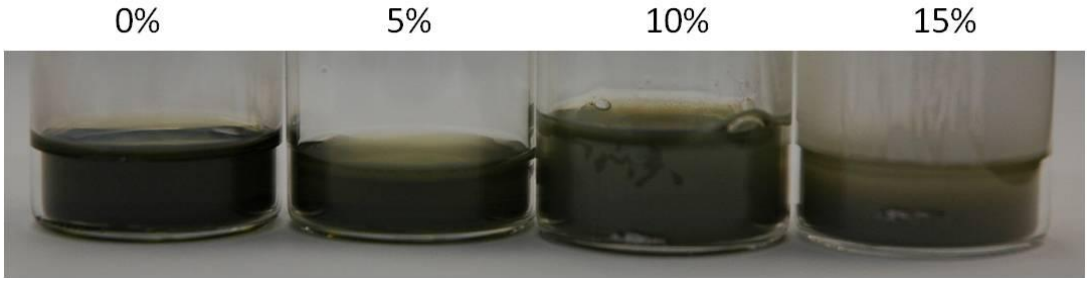

Figure 18: Room temperature cured VE 828-1009F with varied BR content.

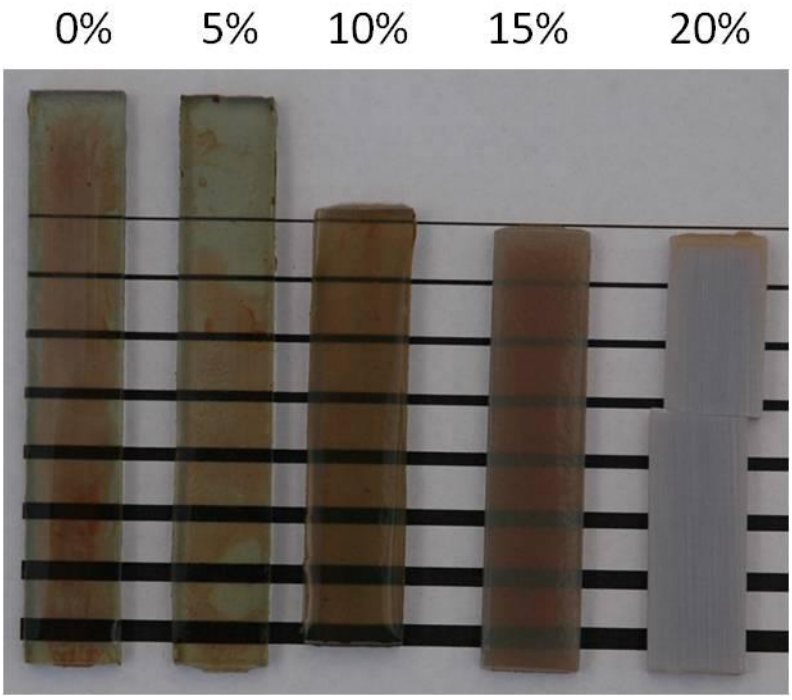

Figure 19: Post cured VE 828 with varied BR content.

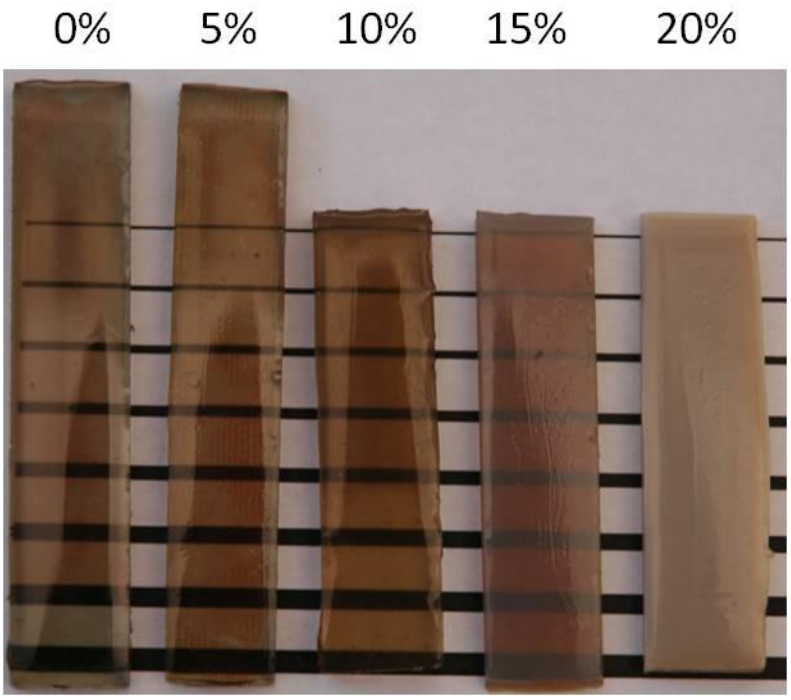

Figure 20: Post cured VE 828-1001F with varied BR content.

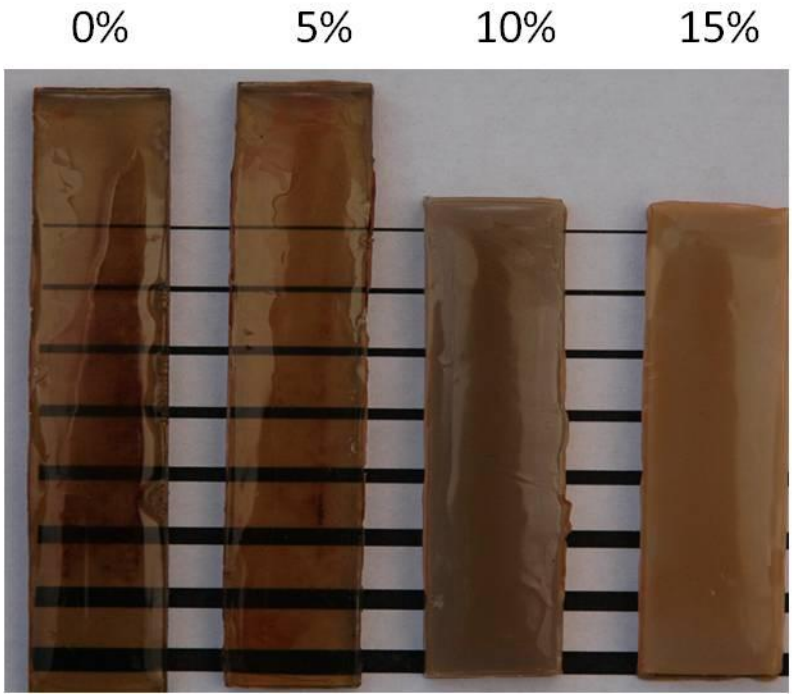

Figure 21: Post cured VE 828-1009F with varied BR content.

Figure 22: Phase separated low styrene content VE 828-1001F.

Figure 23: Phase separated low styrene content VE 828-1009F.

APPENDIX C: Room Temperature to 200°C DMA Plots

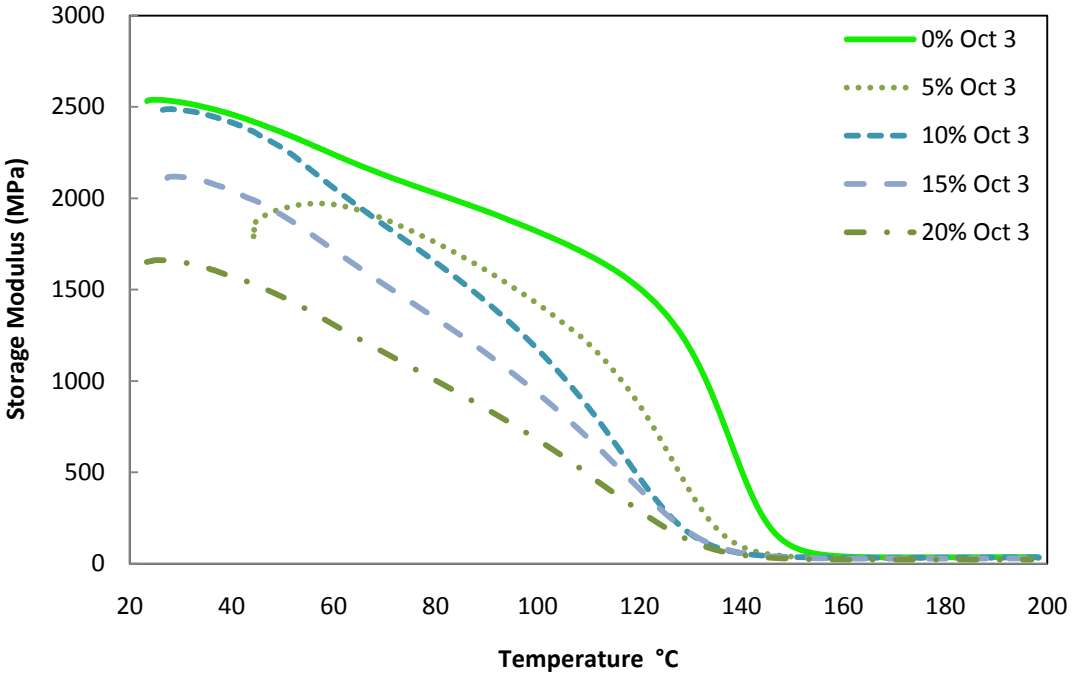

Figure 24: Storage modulus trends for VE 828 with varied BR content.

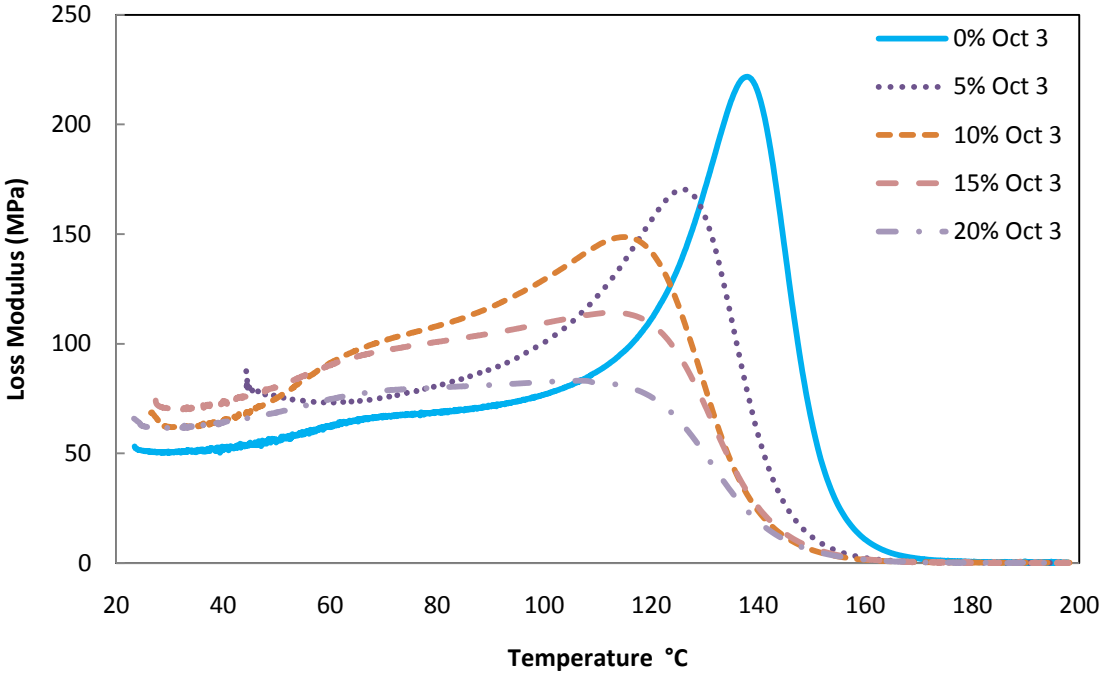

Figure 25: Loss modulus trends for VE 828 with varied BR content.

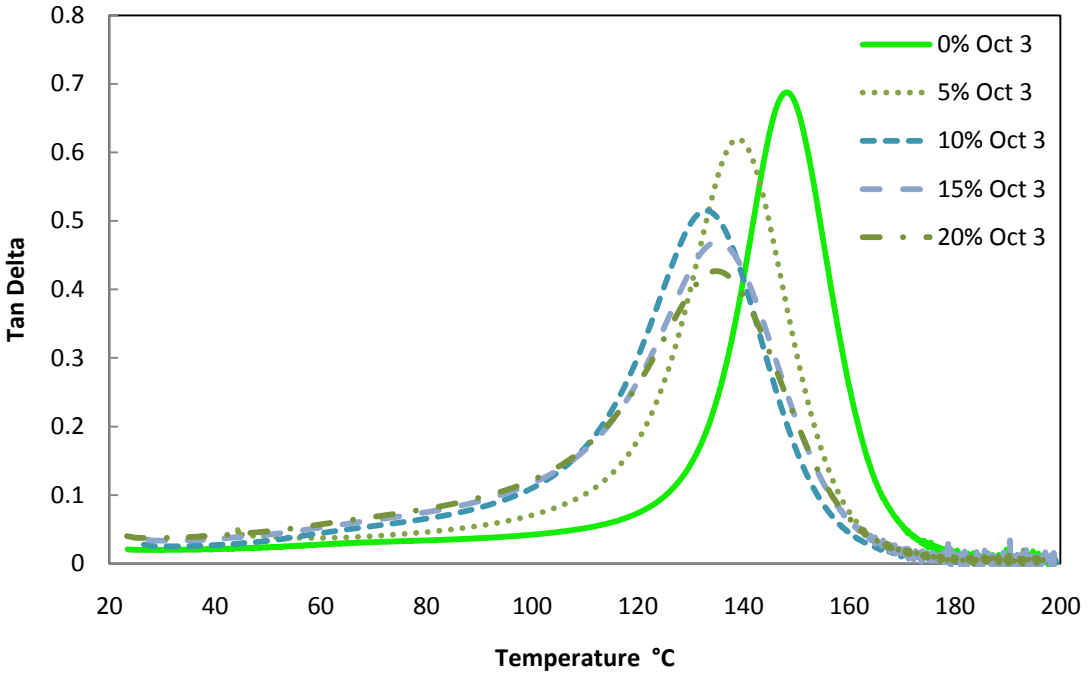

Figure 26: Tan delta trends for VE 828 with varied BR content.

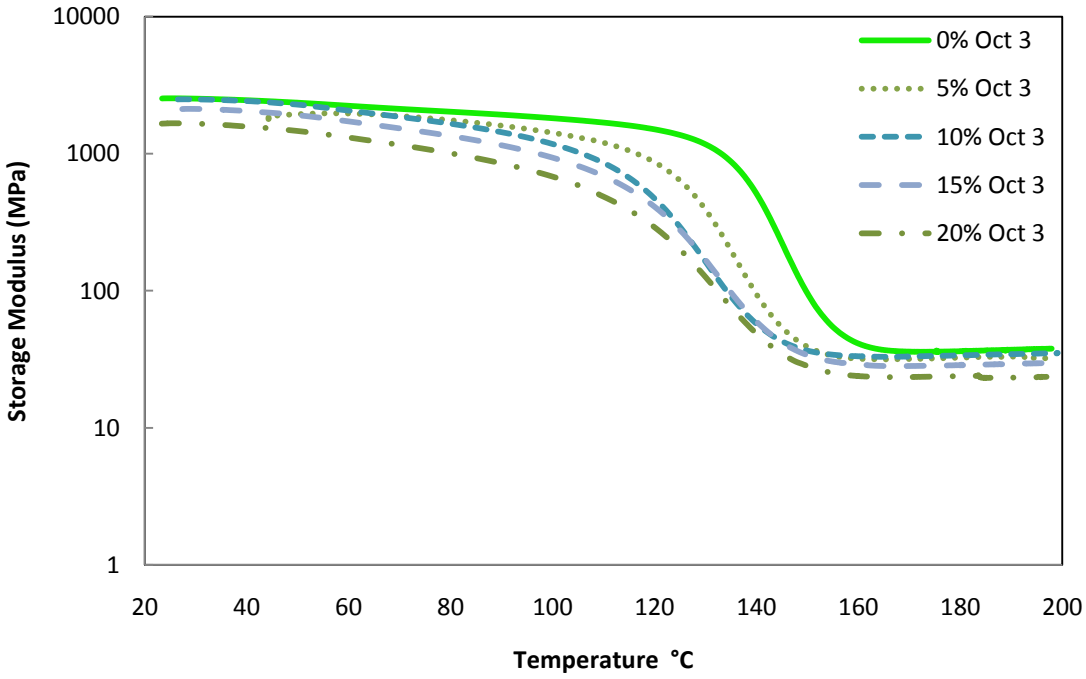

Figure 27: Miscibility trends for VE 828 with varied BR content.

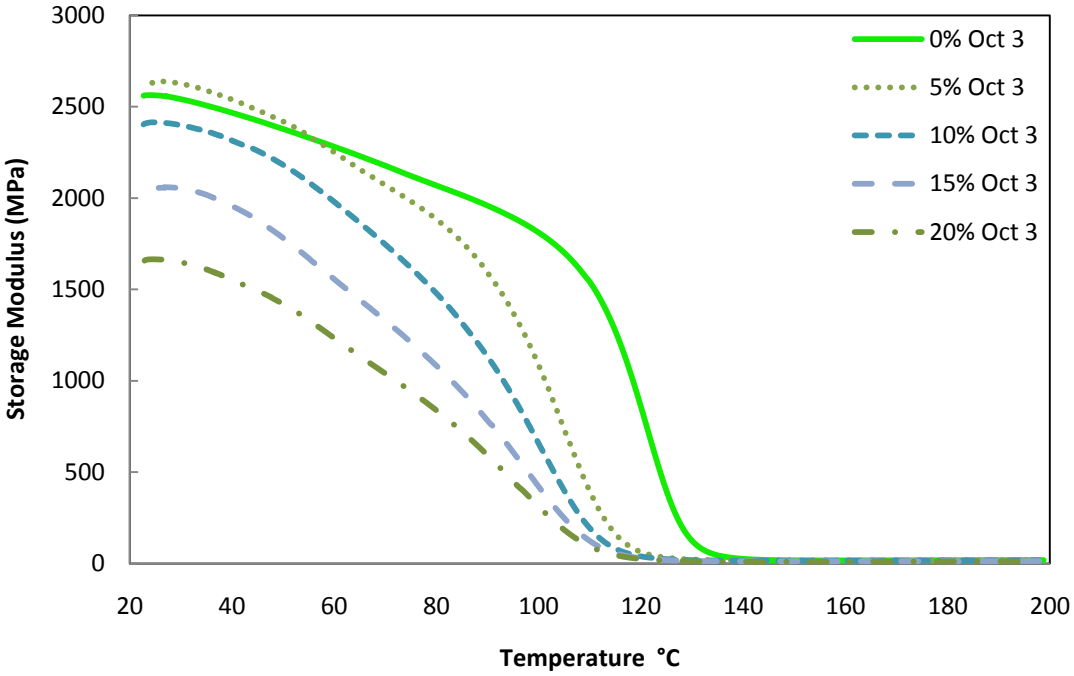

Figure 28: Storage modulus trends for VE 828-1001F with varied BR content.

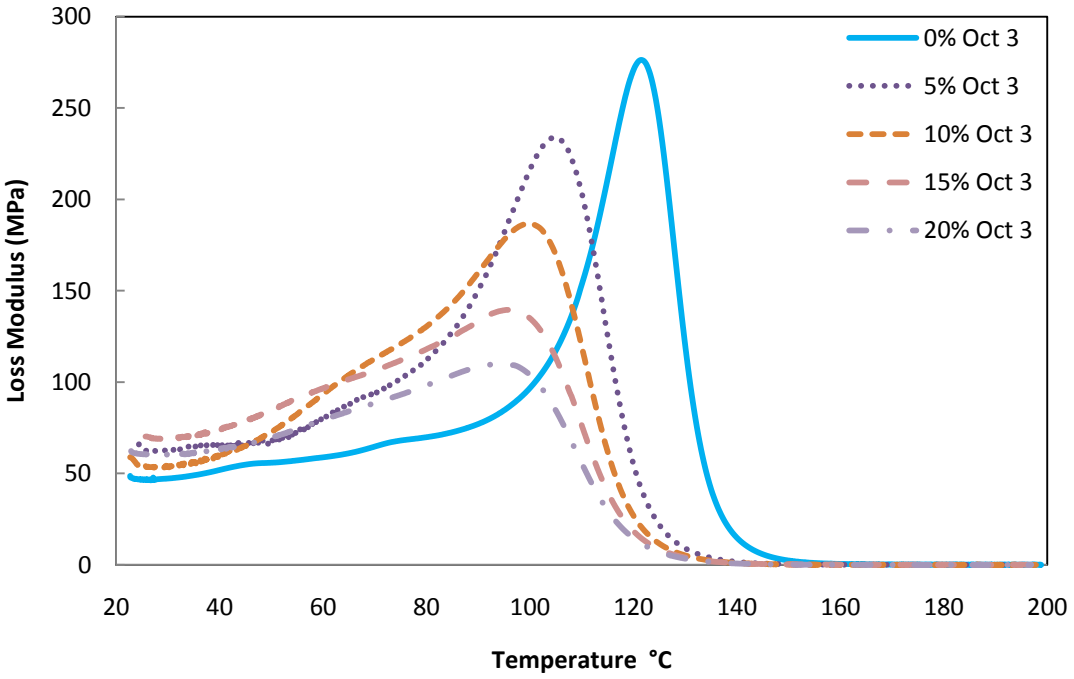

Figure 29: Loss modulus trends for VE 828-1001F with varied BR content.

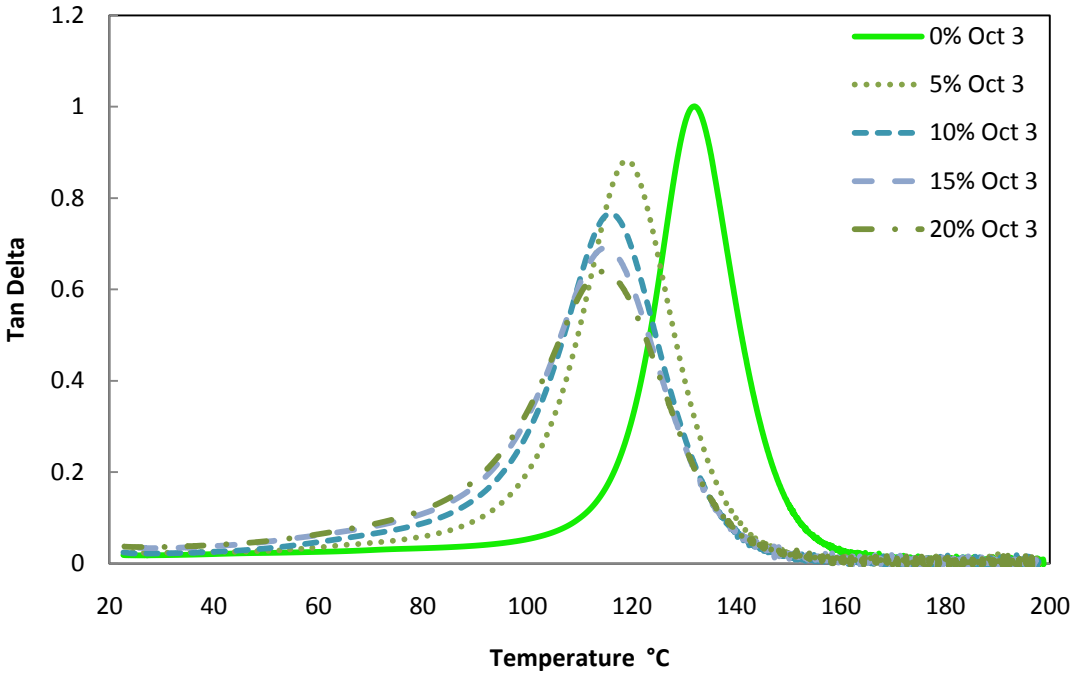

Figure 30: Tan delta trends for VE 828-1001F with varied BR content.

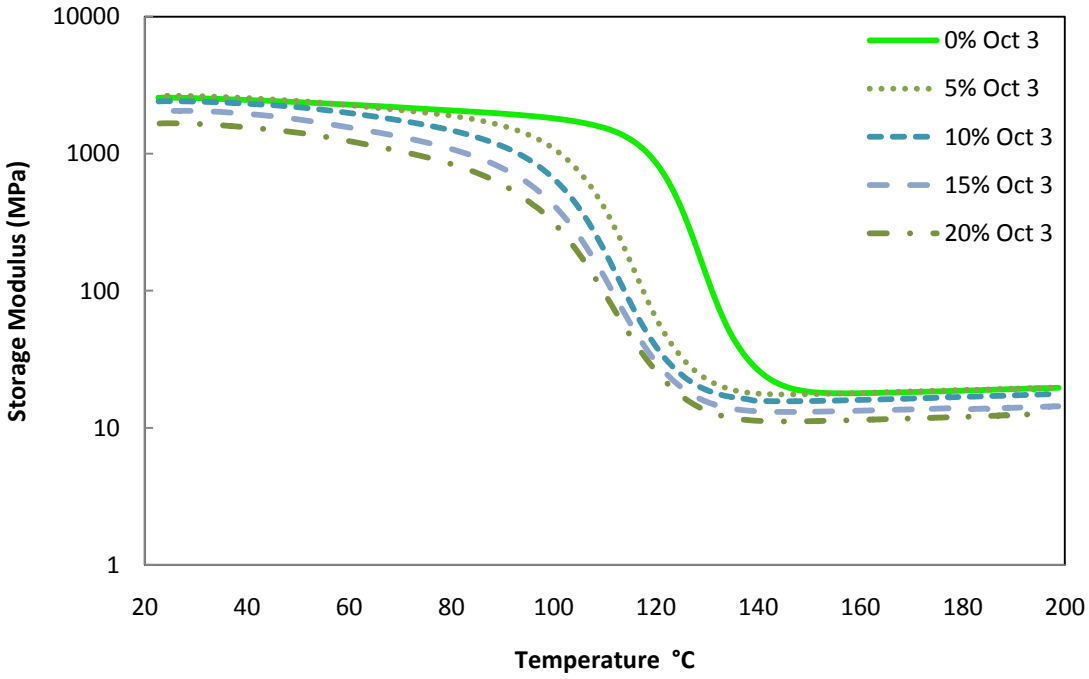

Figure 31: Miscibility trends for VE 828-1001F with varied BR content.

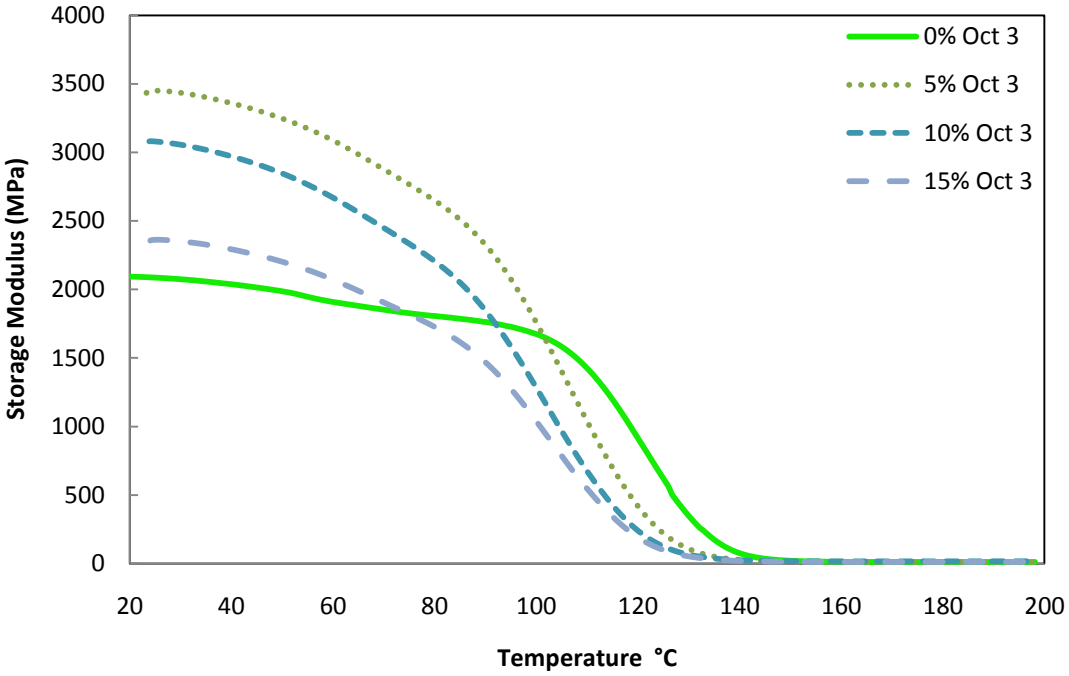

Figure 32: Storage modulus trends for VE 828-1009F with varied BR content.

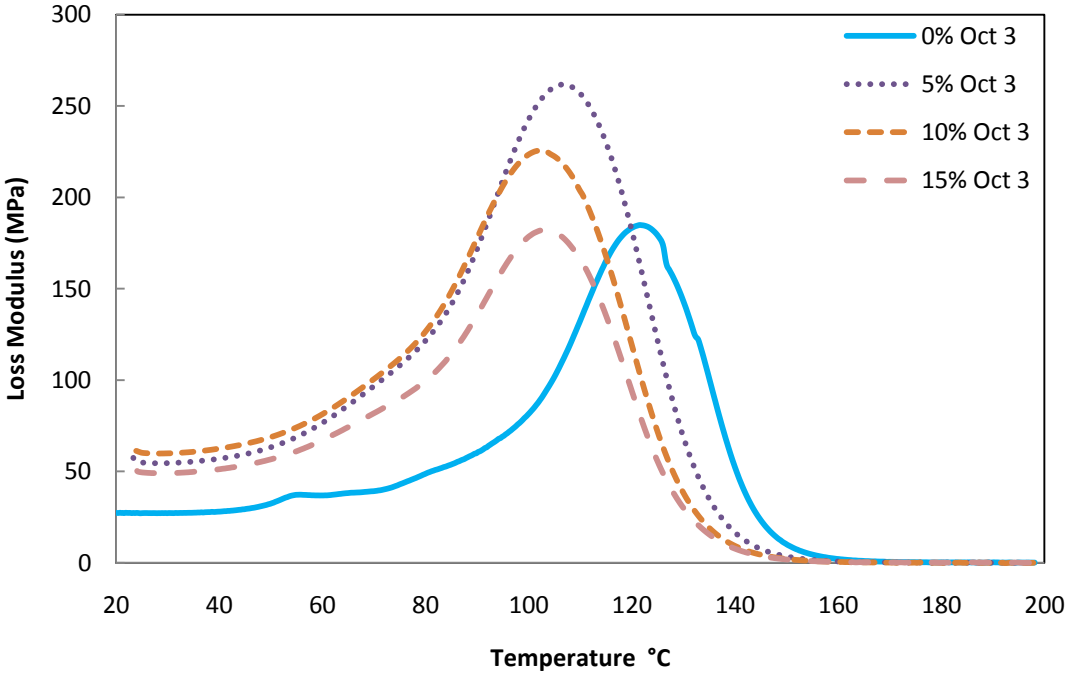

Figure 33: Loss modulus trends for VE 828-1009F with varied BR content.

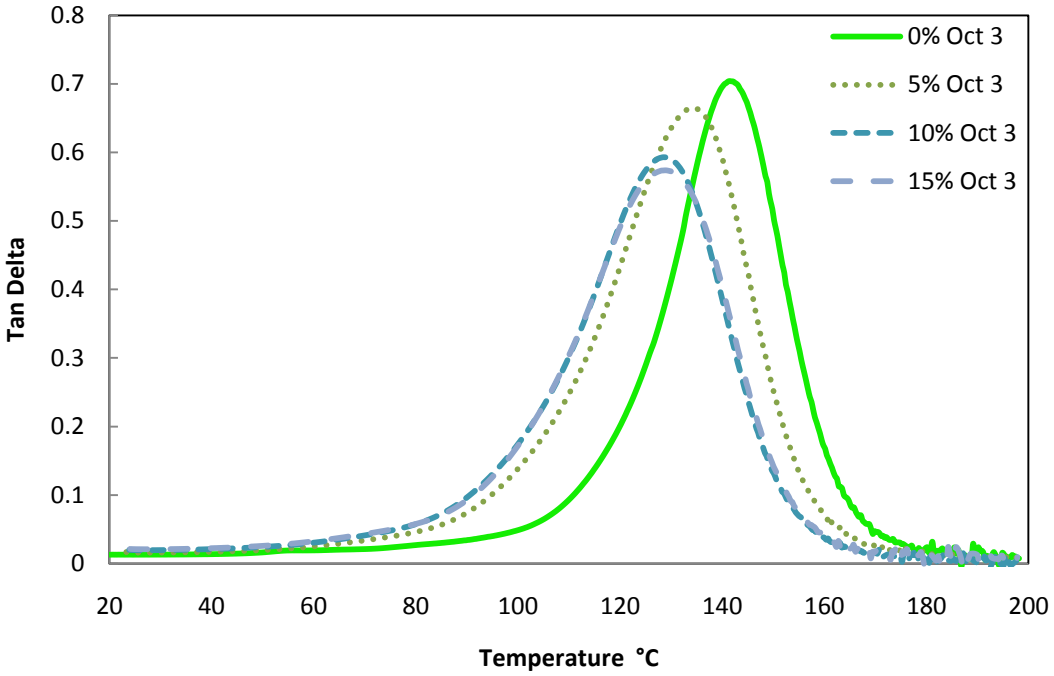

Figure 34: Tan delta trends for VE 828-1009F with varied BR content.

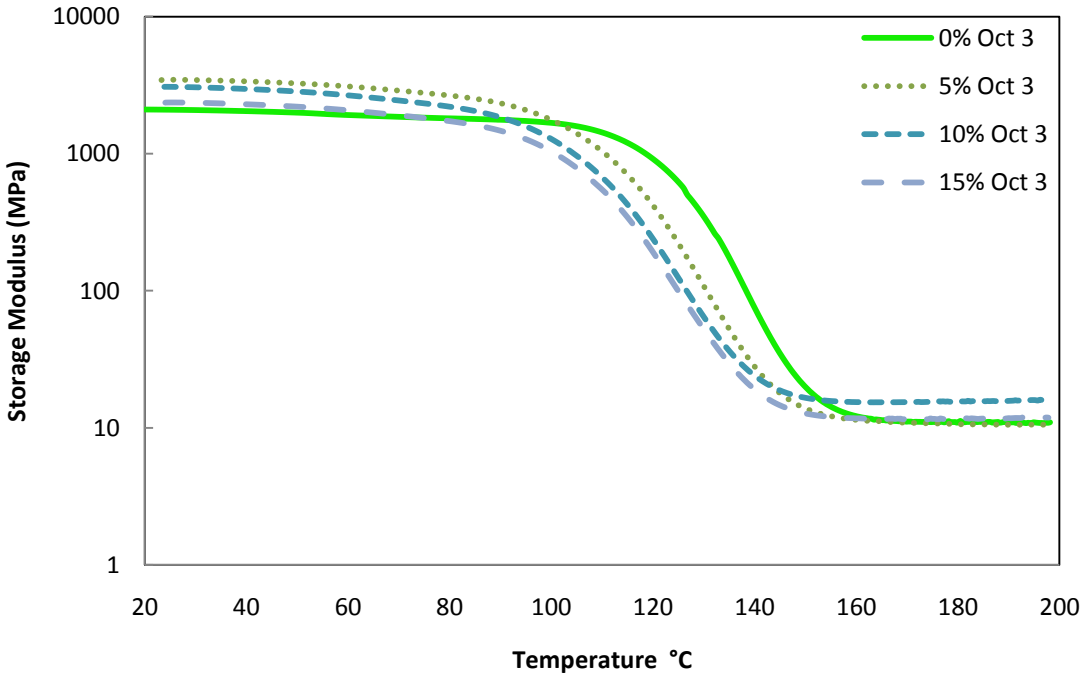

Figure 35: Miscibility trends for VE 828-1009F with varied BR content.

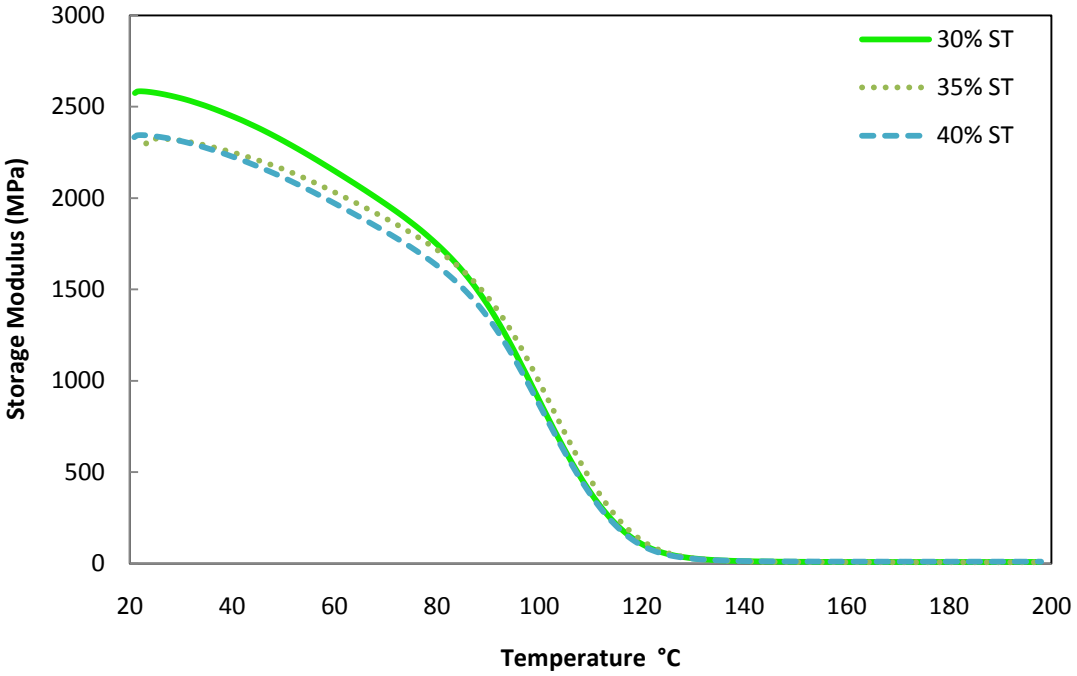

Figure 36: Storage modulus trends for VE 828-1009F BR with varied ST content.

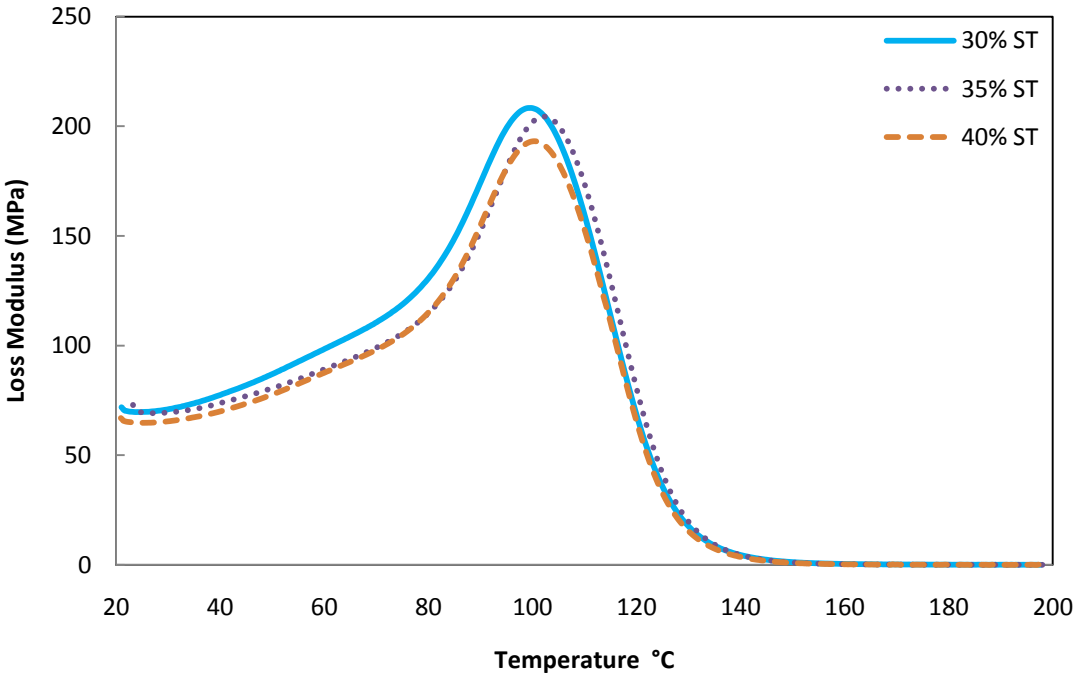

Figure 37: Loss modulus trends for VE 828-1009F BR with varied ST content.

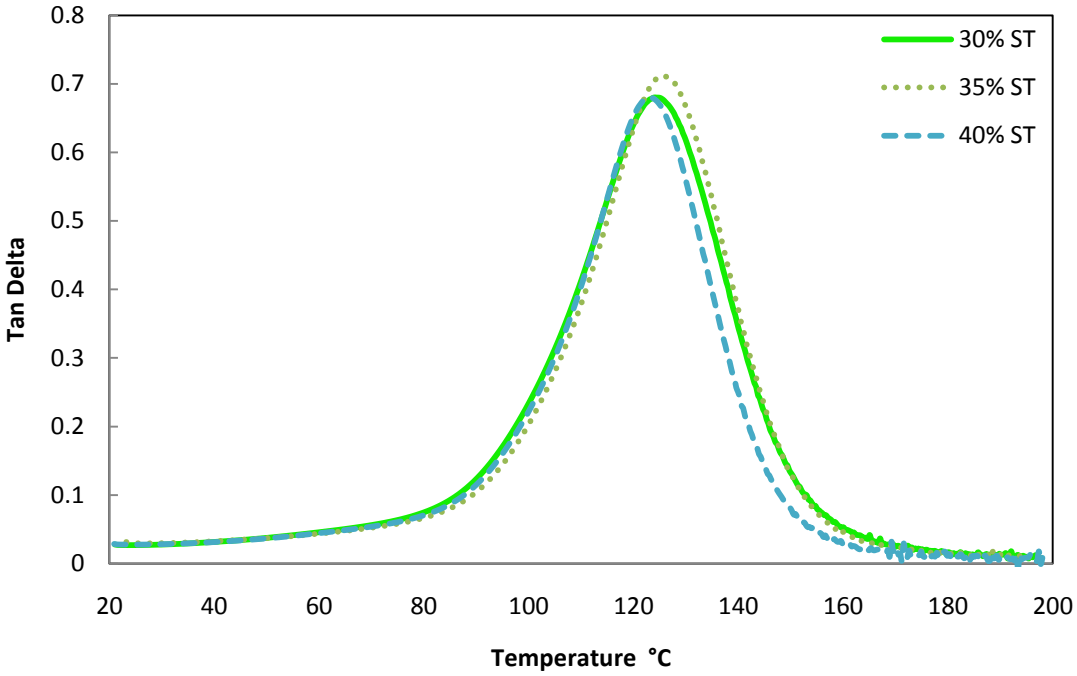

Figure 38: Tan delta trends for VE 828-1009F BR with varied ST content.

APPENDIX D: Low Temperature DMA Plots

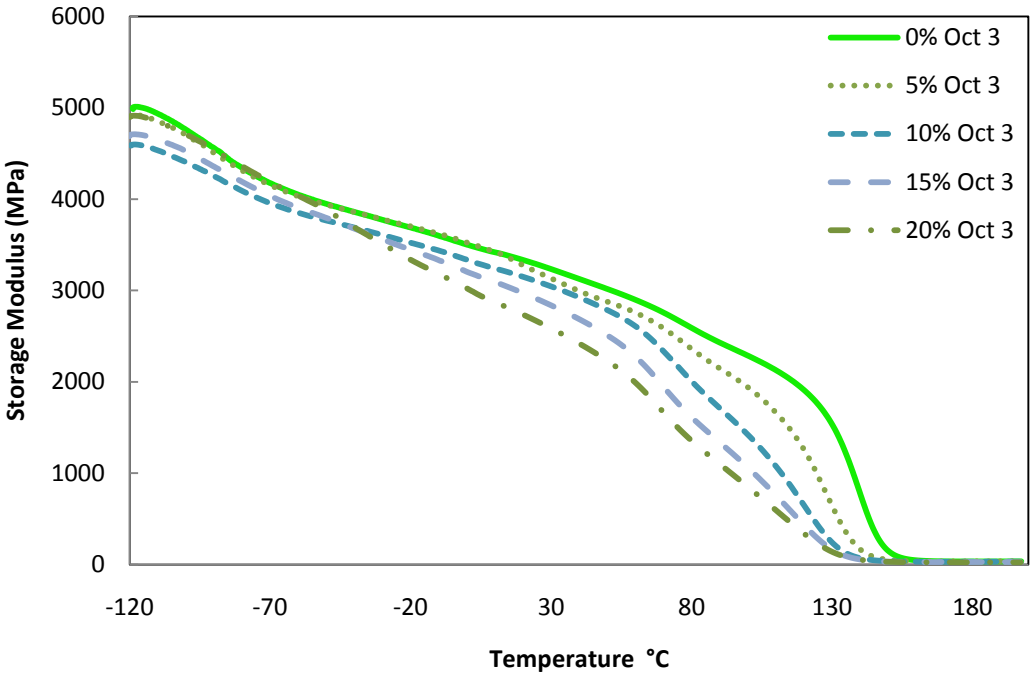

Figure 39: Storage modulus trends for VE 828 with varied BR content.

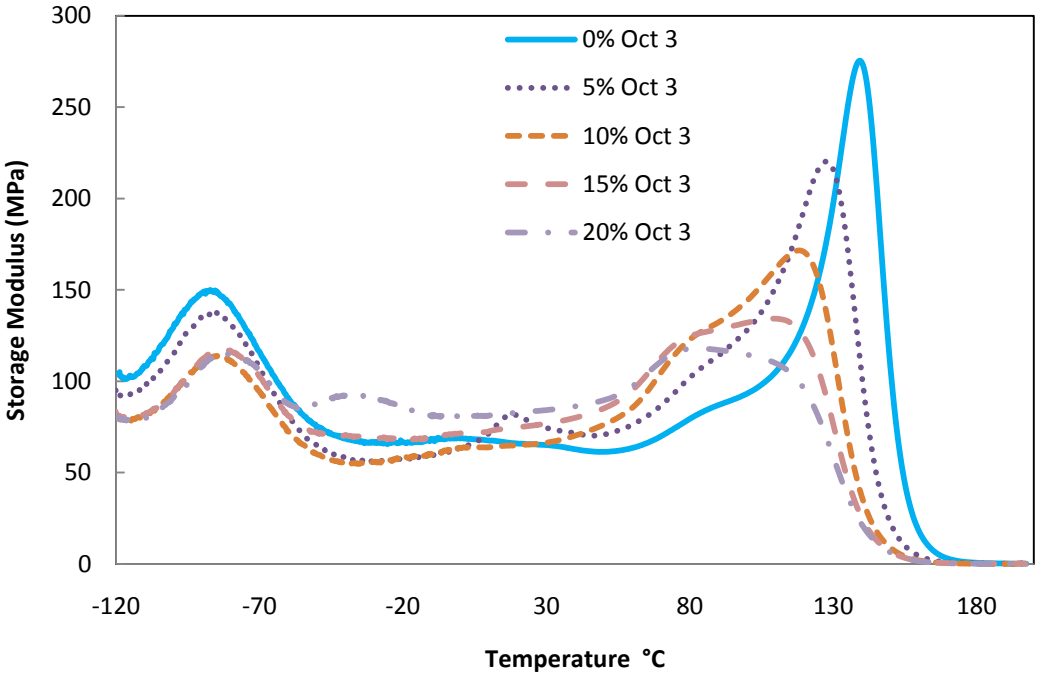

Figure 40: Loss modulus trends for VE 828 with varied BR content.

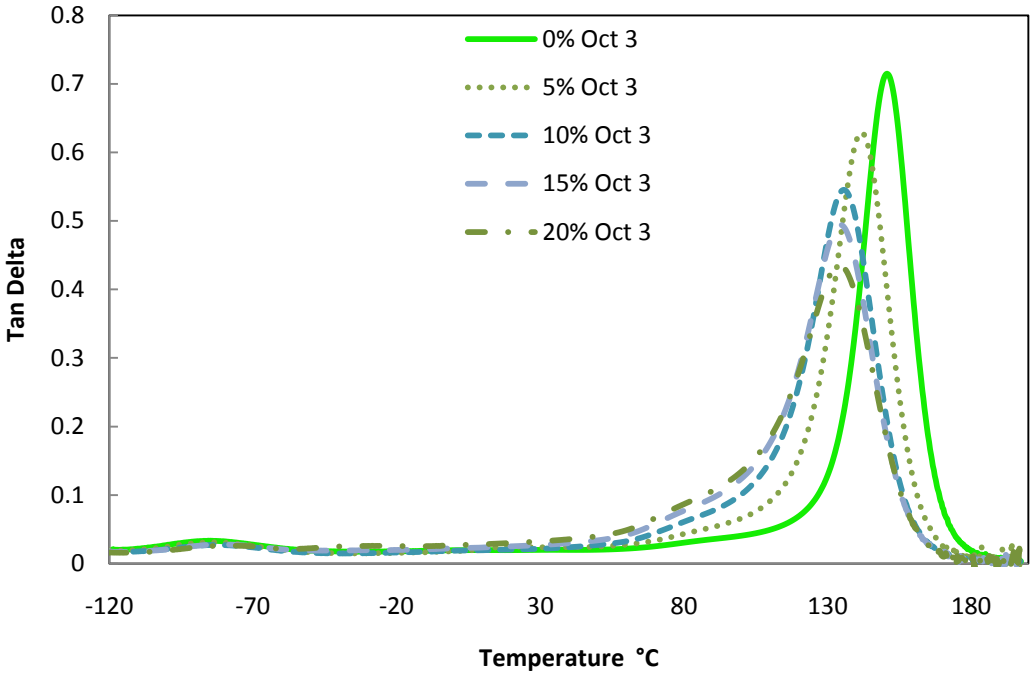

Figure 41: Tan Delta trends for VE 828 with varied BR content.

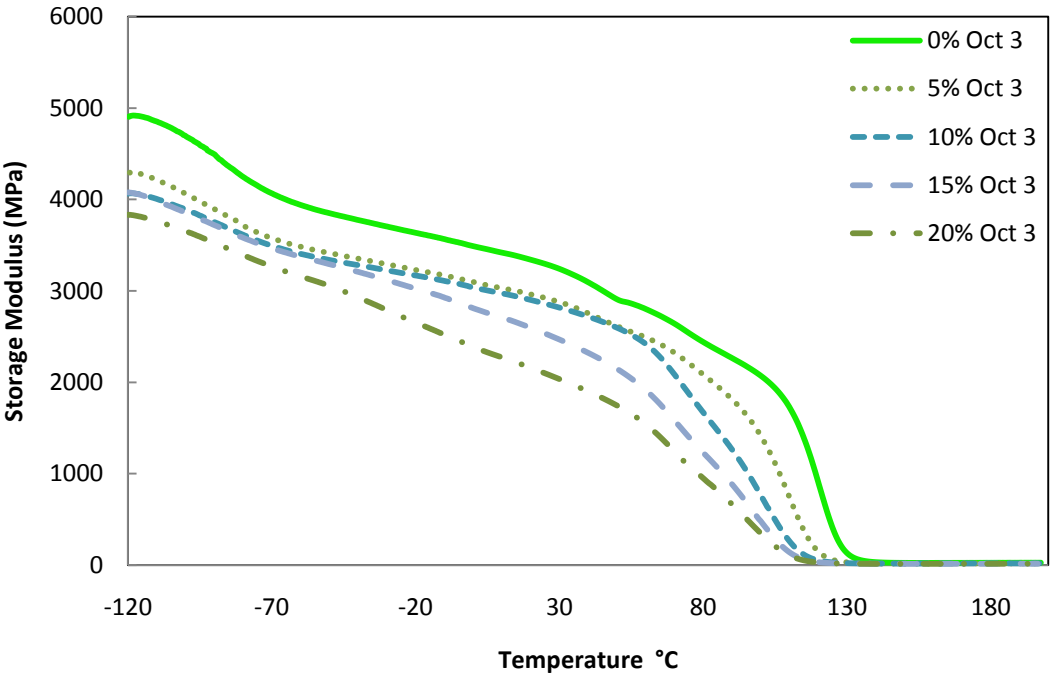

Figure 42: Storage modulus trends for VE 828-1001F with varied BR content.

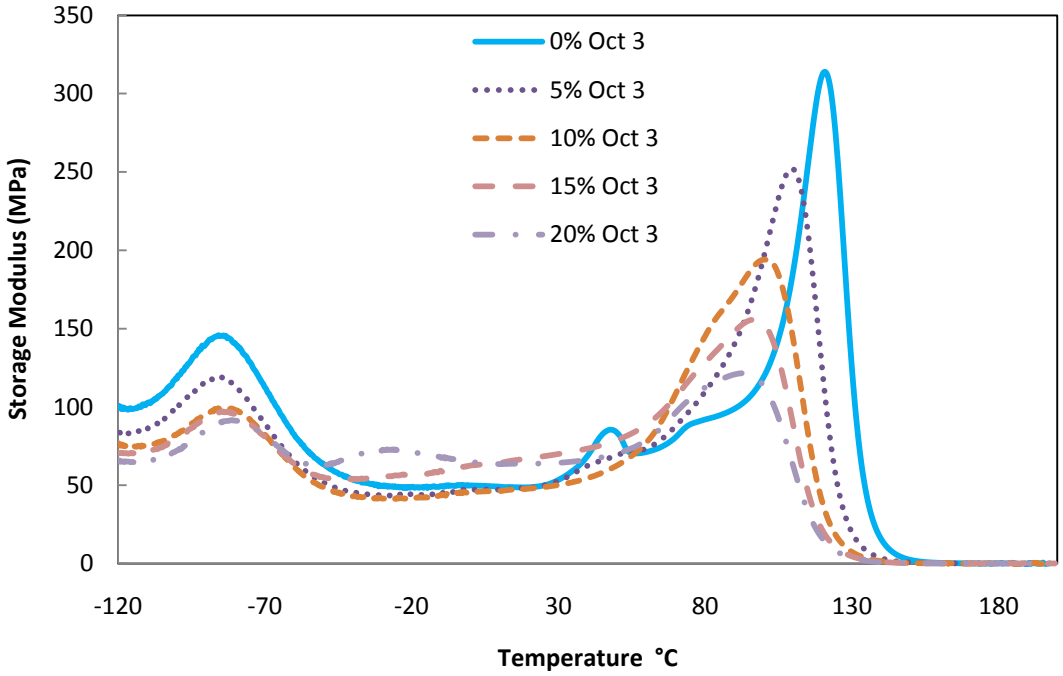

Figure 43: Loss modulus trends for VE 828-1001F with varied BR content.

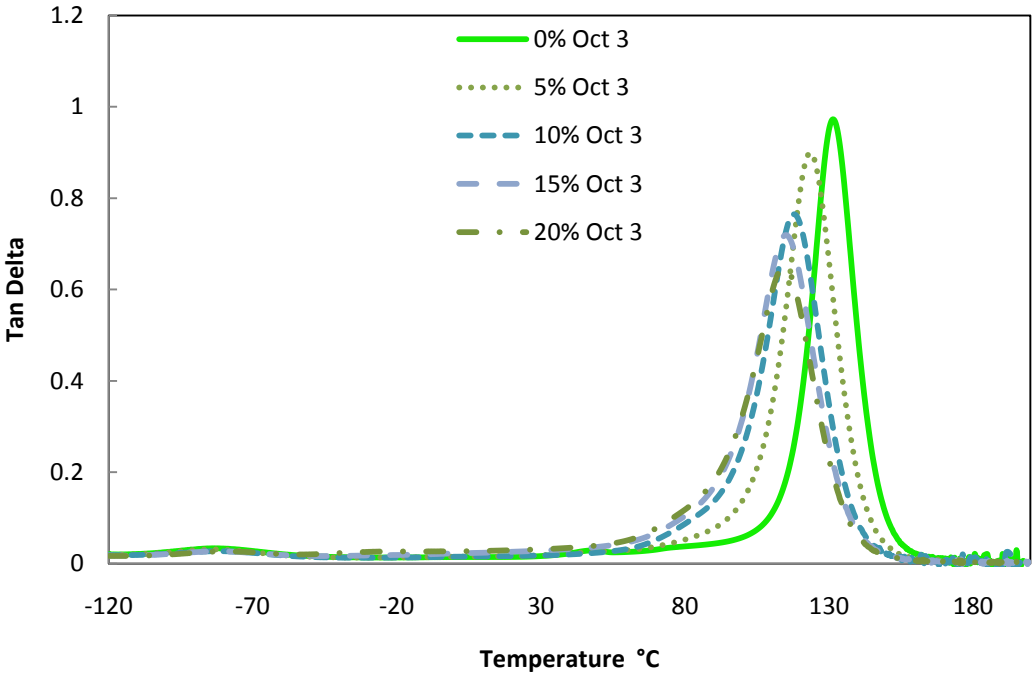

Figure 44: Tan delta trends with VE 828-1001F with varied BR content.

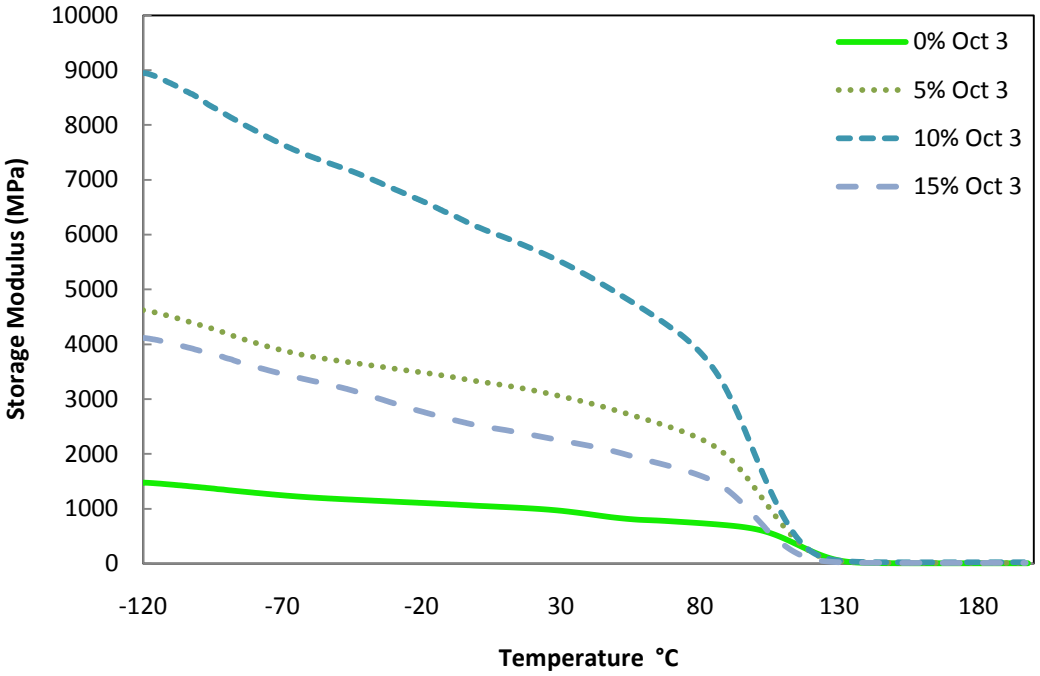

Figure 45: Storage modulus trends for VE 828-1009F with varied BR content.

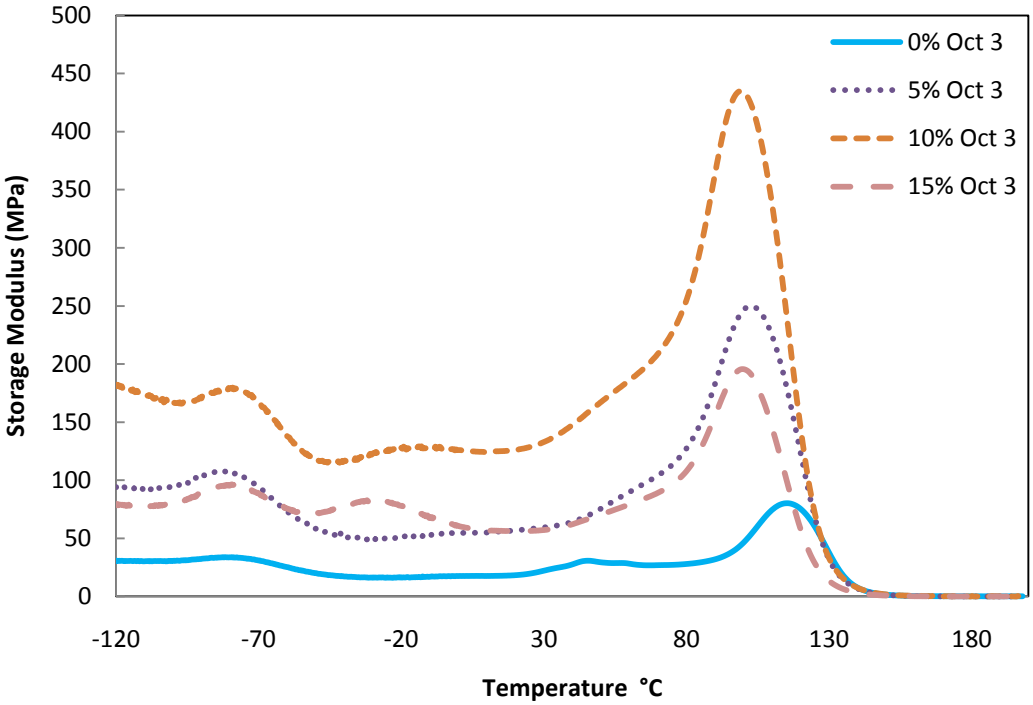

Figure 46: Loss modulus trends for VE 828-1009F with varied BR content.

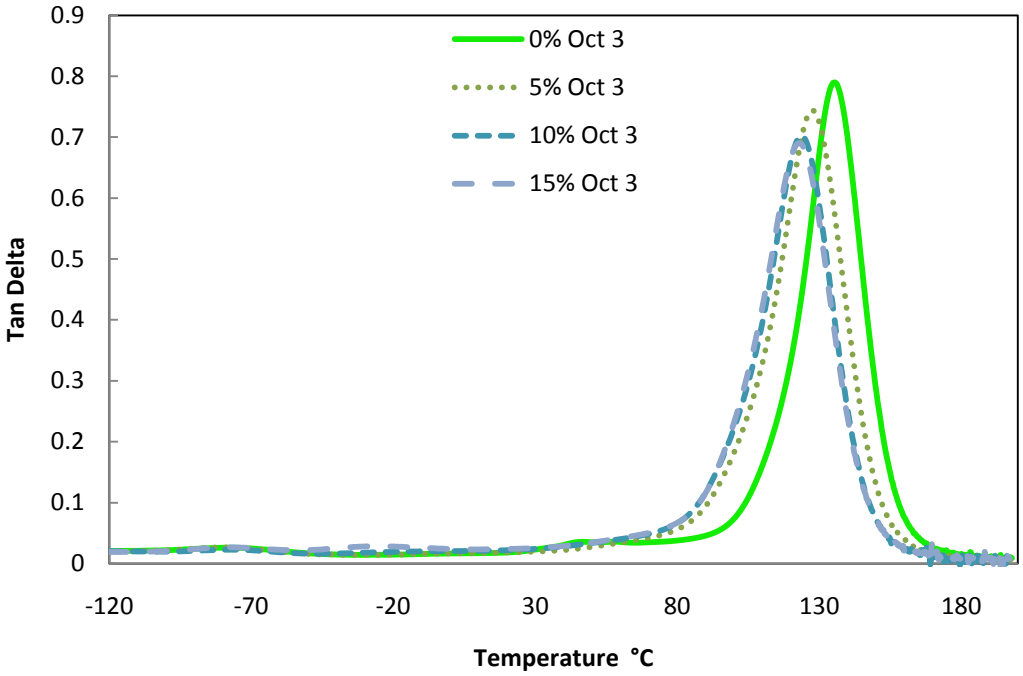

Figure 47: Tan delta trends for VE 828-1009F with varied BR content.

APPENDIX E: Explanation of Correction Displacement Method

Correction displacement method uses the corrected displacement $u_C(P)$ in order to calculate G_{1c}. To determine $u_C(P)$, the indentation displacement $u_i(P)$ and the fracture displacement $u_Q(P)$ are needed. In order to determine $u_i(P)$, the compliance sample must be plotted as and linear curve fitted as seen in Figure 48.

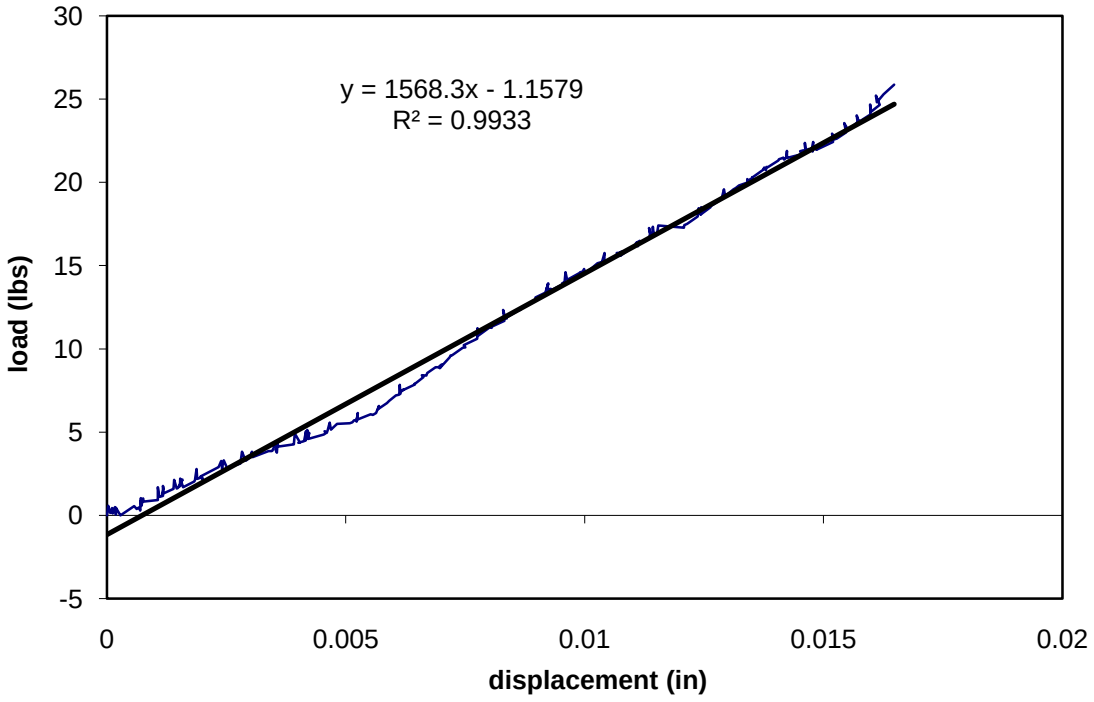

Figure 48: Compliance indentation analysis for VE 828-1009F 15% Oct 3.

The indentation displacement is calculated by using equation 1 where P_Q is the maximum load of the respective sample, b_i is the y-intercept of the indentation compliance and m_i is the slope of the indentation compliance.

$$u_i = \frac{P_Q - b_i}{m_i} \qquad \text{Eq. 1}$$

The corrected displacement is then calculated using equation 2 where u_Q is the displacement at which the sample fractured or at max load.

$$u_C = u_Q - u_i \qquad \text{Eq. 2}$$

The corrected displacement is then used to calculate the energy required to break the sample by using equation 3.

$$U = \frac{1}{2} P_Q u_C \qquad \text{Eq. 3}$$

This corrected energy is used to calculate G_{1C} as outlined in Annex A1.4 of ASTM D 5045. This process must be repeated for each individual sample with each compliance. Additional data can be found in Appendix F for all samples.

APPENDIX F: Supplemental Fracture Toughness Data

Table 7: VE 828 0% Oct 3 fracture toughness sample data.

Compliance 1 (1)			Slope	Y-int.		Compliance 2 (2)	Slope	Y-int.
			2277	-0.3535			2277	-0.3535
	B	W	W-a	Load (lb_F)	Disp. (in.)	K_{1c} ($MPa\text{-}m^{1/2}$)	G_{1c} (J/m^2) (1)	G_{1c} (J/m^2) (2)
1	0.245	0.482	0.252	12.24368	0.011740	0.78	218	220
2	0.244	0.49	0.247	10.19332	0.008750	0.69	124	127
3	0.248	0.489	0.253	14.13948	0.011326	0.90	198	200
4	0.246	0.486	0.262	15.51609	0.012039	0.94	215	216

Table 8: VE 828 5% Oct 3 fracture toughness sample data.

Compliance 1 (1)			Slope	Y-int.		Compliance 2 (2)	Slope	Y-int.
			2039.3	-1.2276			1896.4	0.6941
	B	W	W-a	Load (lb_F)	Disp. (in.)	K_{1c} ($MPa\text{-}m^{1/2}$)	G_{1c} (J/m^2) (1)	G_{1c} (J/m^2) (2)
1	0.243	0.48	0.248	11.52461	0.011763	0.76	187	205
2	0.249	0.483	0.245	12.75616	0.012191	0.84	198	216
3	0.245	0.485	0.245	13.0354	0.01542	0.88	325	344
4	0.245	0.481	0.246	14.48894	0.012079	0.96	186	205

Table 9: VE 828-1001F 0% Oct 3 fracture toughness sample data.

Compliance 1 (1)			Slope	Y-int.		Compliance 2 (2)	Slope	Y-int.
			2189.4	-0.0053			2228.4	-0.0016
	B	W	W-a	Load (lb_F)	Disp. (in.)	K_{1c} ($MPa\text{-}m^{1/2}$)	G_{1c} (J/m^2) (1)	G_{1c} (J/m^2) (2)
1	0.243	0.497	0.271	14.85193	0.012281	0.88	218	223
2	0.24	0.49	0.277	18.8366	0.014917	1.08	312	320
3	0.249	0.496	0.272	17.65946	0.014883	1.02	312	318
4	0.248	0.492	0.269	16.09097	0.012903	0.94	235	241

Table 10: VE 828-1001F 5% Oct 3 fracture toughness sample data.

Compliance 1 (1)			Slope	Y-int.		Compliance 2 (2)	Slope	Y-int.
			2264	0.1988			2177.7	0.0344
	B	W	W-a	Load (lb_F)	Disp. (in.)	K_{1c} ($MPa\text{-}m^{1/2}$)	G_{1c} (J/m^2) (1)	G_{1c} (J/m^2) (2)
1	0.247	0.493	0.255	16.72822	0.015401	1.07	381	364
2	0.249	0.488	0.25	18.03553	0.018214	1.17	531	511
3	0.248	0.49	0.25	14.15686	0.01188	0.92	232	219
4	0.246	0.498	0.26	16.53072	0.013991	1.04	310	293

Table 11: VE 828-1009F 0% Oct 3 fracture toughness sample data.

Compliance 1 (1)			Slope	Y-int.		Compliance 2 (2)	Slope	Y-int.
			2116.1	-0.3928			2153.4	-0.8519
	B	W	W-a	Load (lb_F)	Disp. (in.)	K_{1c} ($MPa\text{-}m^{1/2}$)	G_{1c} (J/m^2) (1)	G_{1c} (J/m^2) (2)
1	0.239	0.49	0.265	16.28913	0.012837	1.01	224	221
2	0.243	0.488	0.267	16.79212	0.015173	1.00	321	317
3	0.238	0.487	0.262	16.46792	0.013917	1.03	277	273
4	0.241	0.492	0.268	18.50456	0.015465	1.12	329	326

Table 12: VE 828-1009F 5% Oct 3 fracture toughness sample data.

Compliance 1 (1)			Slope	Y-int.		Compliance 2 (2)	Slope	Y-int.
			1896	-0.9843			2146.2	-1.5844
	B	W	W-a	Load (lb_F)	Disp. (in.)	K_{1c} ($MPa\text{-}m^{1/2}$)	G_{1c} (J/m^2) (1)	G_{1c} (J/m^2) (2)
1	0.252	0.496	0.246	17.95404	0.015002	1.20	258	304
2	0.25	0.492	0.242	21.38485	0.021026	1.46	581	650
3	0.25	0.488	0.249	16.29522	0.015734	1.06	307	348
4	0.247	0.488	0.246	17.60193	0.017205	1.18	381	425

Table 13: VE 828-1009F 10% Oct 3 fracture toughness sample data.

Compliance 1 (1)			Slope	Y-int.		Compliance 2 (2)	Slope	Y-int.
			1730.8	-1.1437			1637	-1.1624
	B	W	W-a	Load (lb_F)	Disp. (in.)	K_{1c} (MPa-$m^{1/2}$)	G_{1c} (J/m^2) (1)	G_{1c} (J/m^2) (2)
1	0.247	0.488	0.253	25.58899	0.02538	1.64	720	655
2	0.249	0.494	0.256	26.10225	0.026055	1.65	748	682
3	0.249	0.496	0.256	26.32579	0.025079	1.67	674	606
4	0.248	0.49	0.258	32.08668	0.029912	1.99	949	851

Table 14: VE 828-1009F 15% Oct 3 fracture toughness sample data.

Compliance 1 (1)			Slope	Y-int.		Compliance 2 (2)	Slope	Y-int.
			1735.8	-7.36			1568.3	-1.1579
	B	W	W-a	Load (lb_F)	Disp. (in.)	K_{1c} (MPa-$m^{1/2}$)	G_{1c} (J/m^2) (1)	G_{1c} (J/m^2) (2)
1	0.247	0.477	0.247	23.12034	0.026563	1.50	604	744
2	0.251	0.495	0.273	29.11542	0.032633	1.65	866	993
3	0.251	0.5	0.267	28.77164	0.027736	1.71	524	655
4	0.249	0.497	0.266	31.92639	0.03281	1.91	865	995

Table 15: VE 828-1009F Oct 3 40% Styrene fracture toughness sample data.

Compliance 1 (1)			Slope	Y-int.		Compliance 2 (2)	Slope	Y-int.
			1901.7	-0.571			2114.9	-4.2171
	B	W	W-a	Load (lb_F)	Disp. (in.)	K_{1c} (MPa-$m^{1/2}$)	G_{1c} (J/m^2) (1)	G_{1c} (J/m^2) (2)
1	0.224	0.447	0.23	16.66124	0.018840	1.24	561	514
2	0.225	0.44	0.23	13.19995	0.02087	0.96	615	570
3	0.227	0.448	0.227	17.56942	0.020584	1.32	669	622
4	0.224	0.445	0.225	14.9017	0.01616	1.15	421	374

APPENDIX G: Additional SEM Micrographs

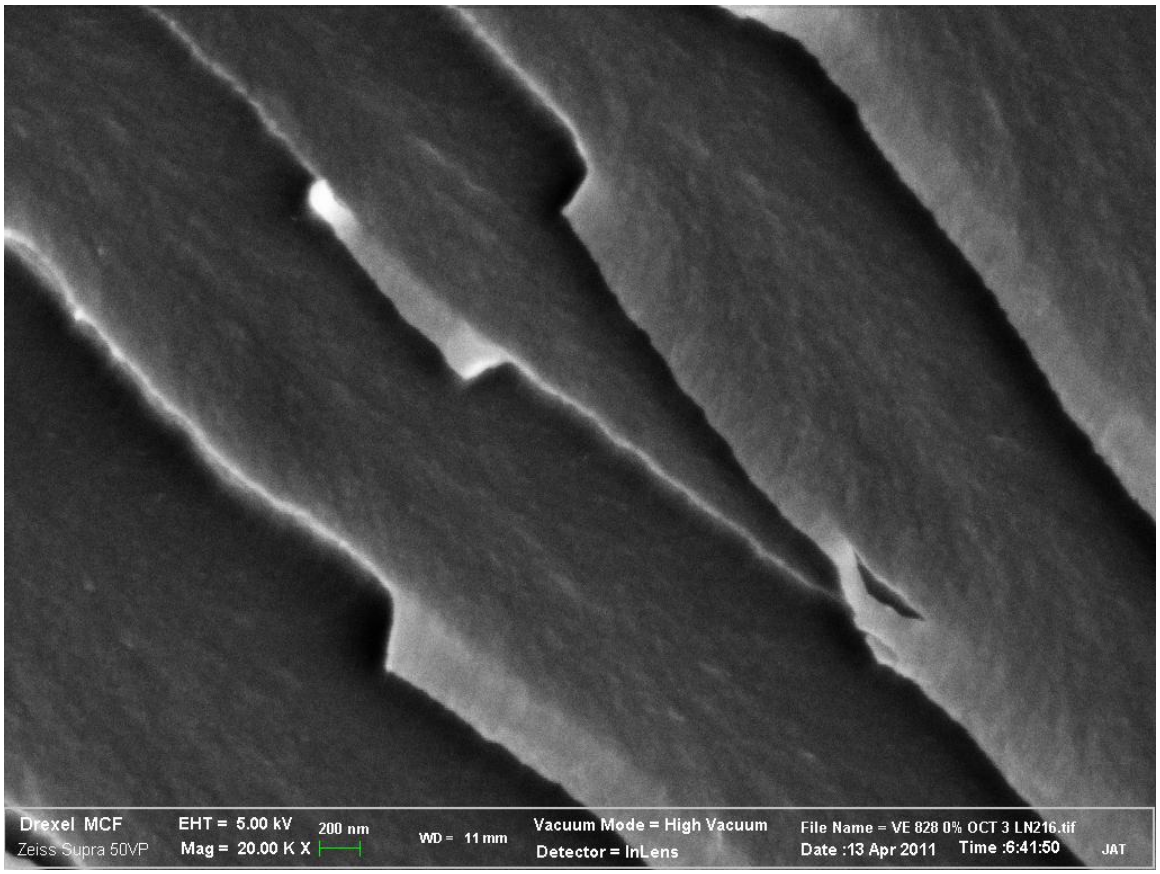

Figure 49: LN2 prepared VE 828 0% Oct 3.

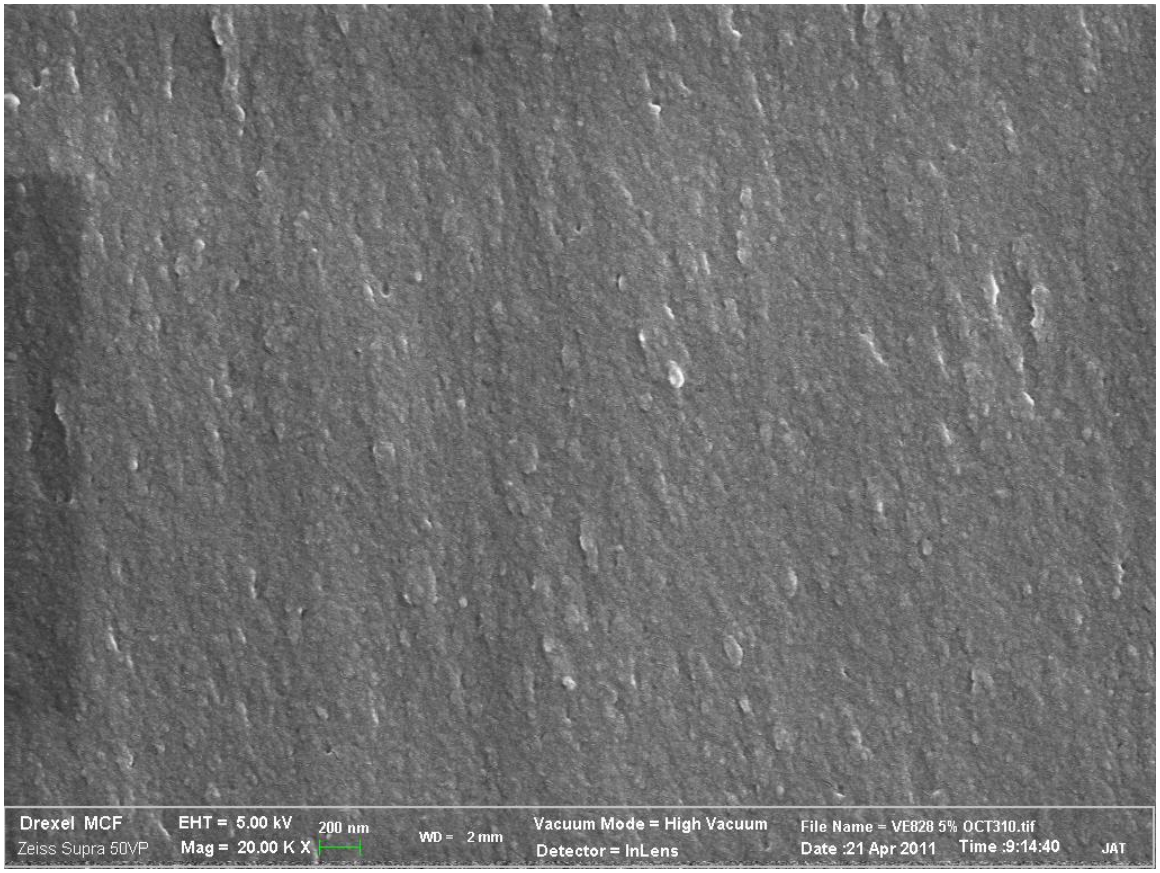

Figure 50: LN2 prepared VE 828 5% Oct 3.

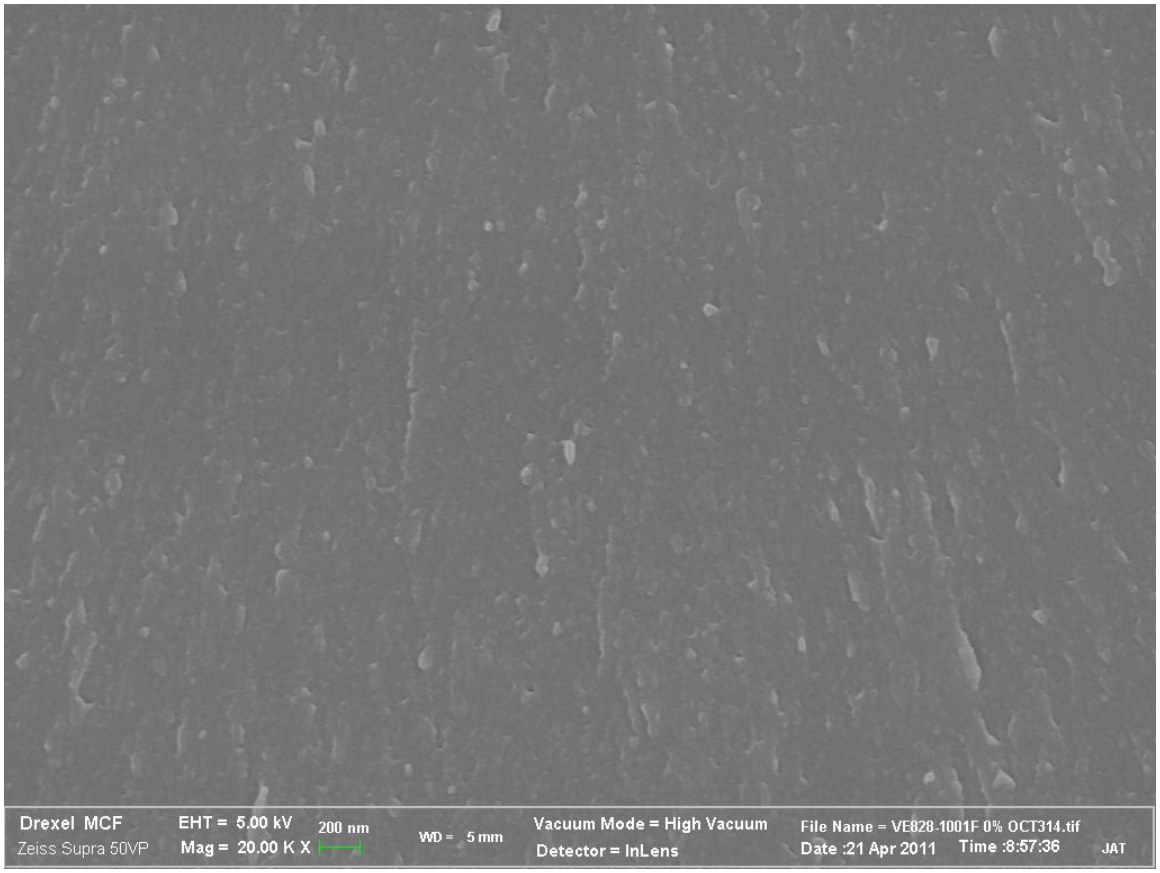

Figure 51: LN2 prepared VE 828-1009F 0% Oct 3.

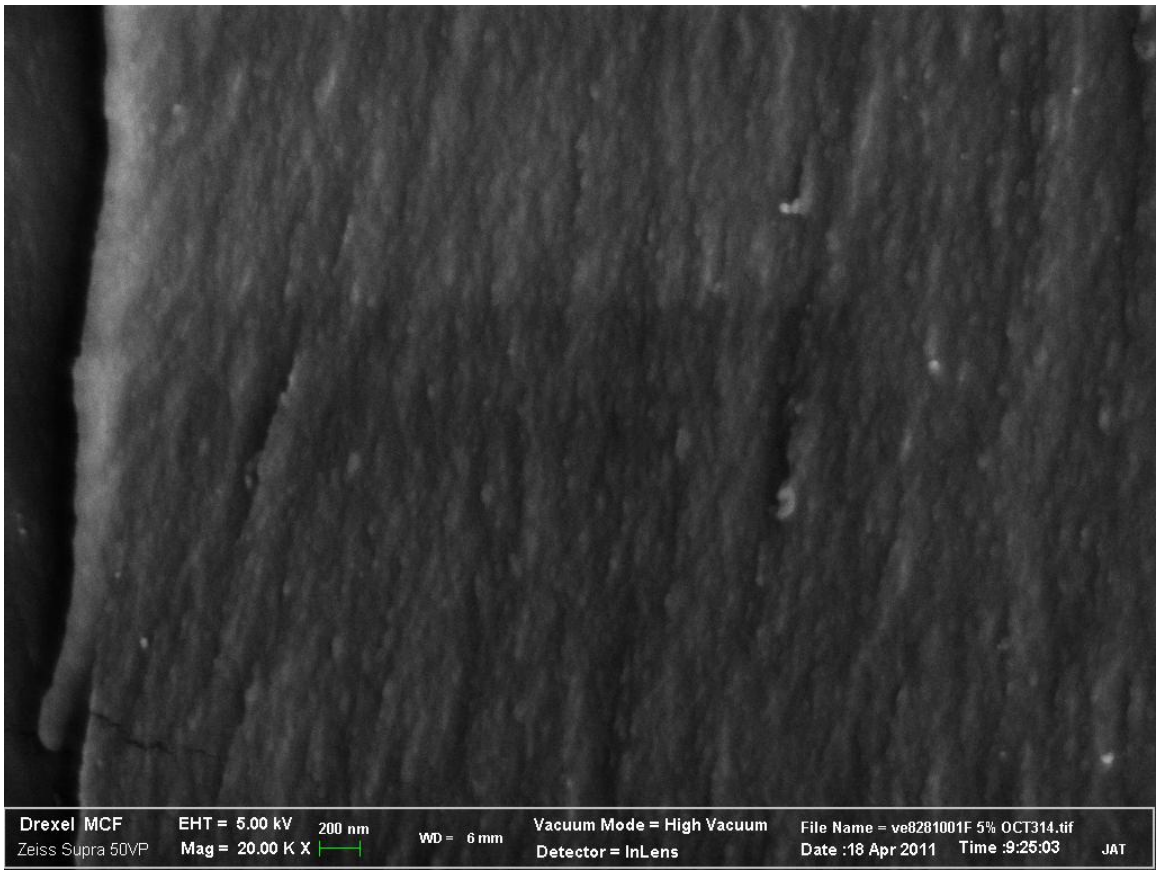

Figure 52: LN2 prepared VE 828-1001F 5% Oct 3.

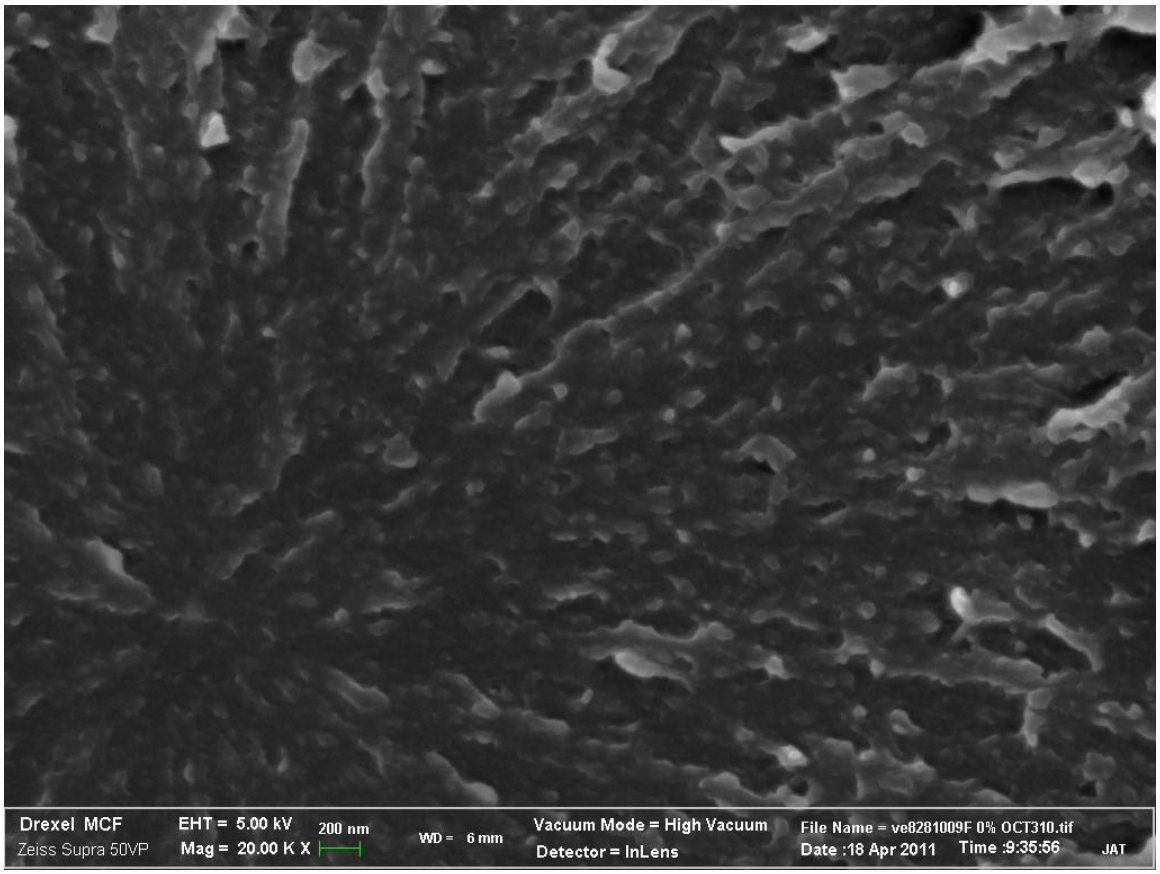

Figure 53: LN2 prepared VE 828-1009F 0% Oct 3.

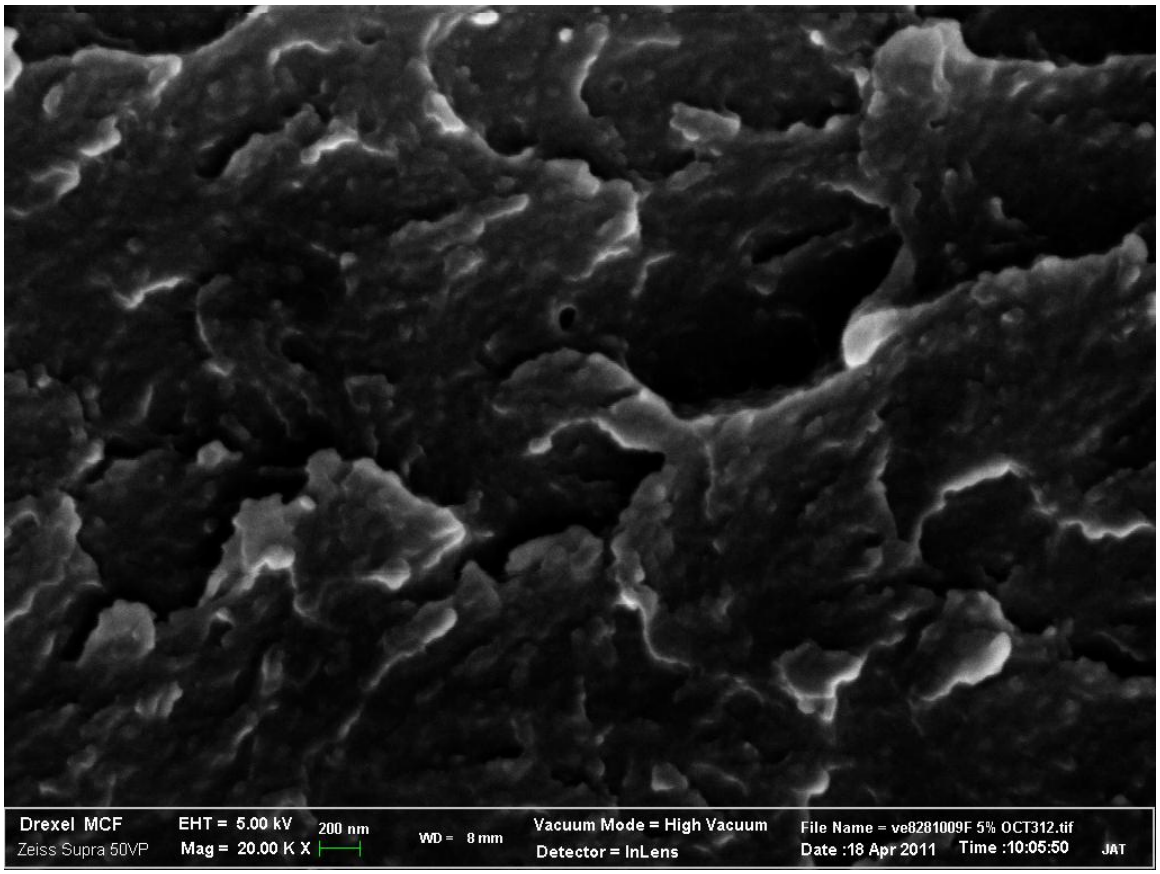

Figure 54: LN2 prepared VE 828-1009F 5% Oct 3.

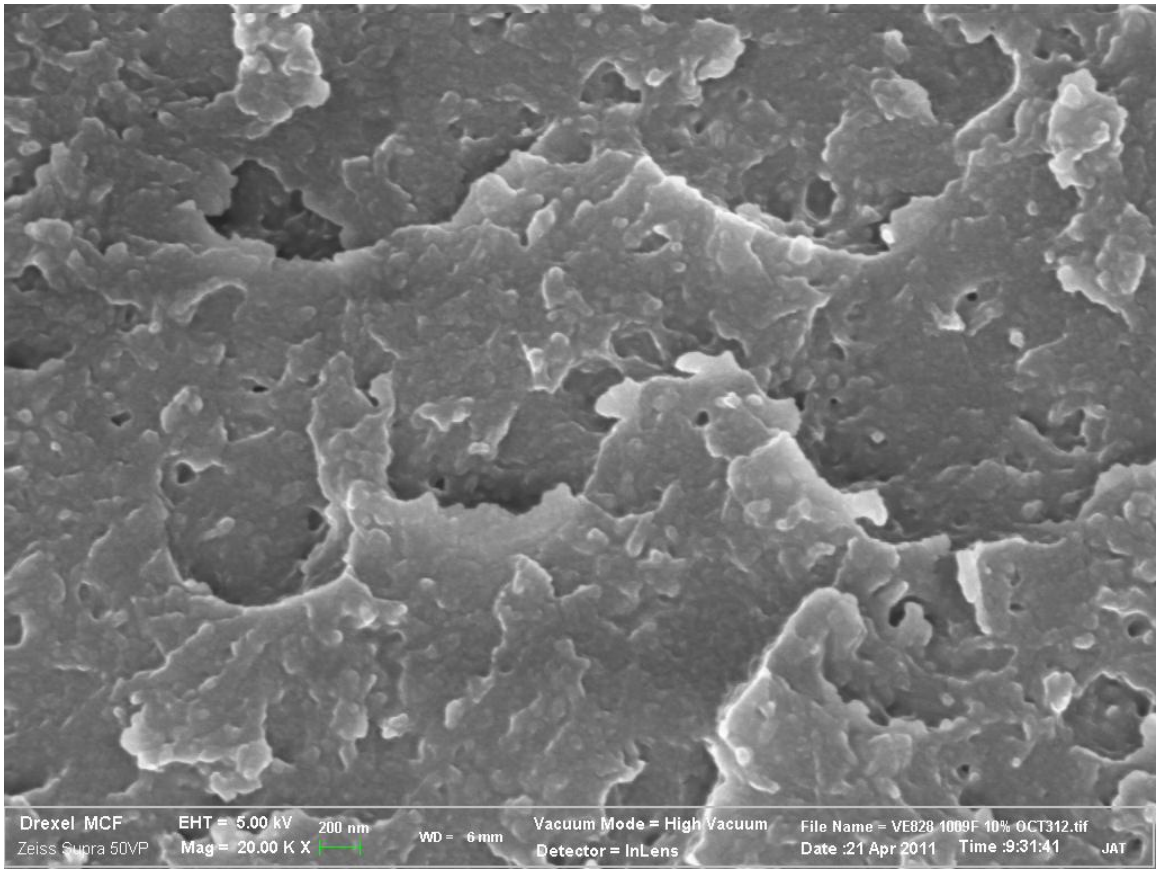

Figure 55: LN2 prepared VE 828-1009F 10% Oct 3.

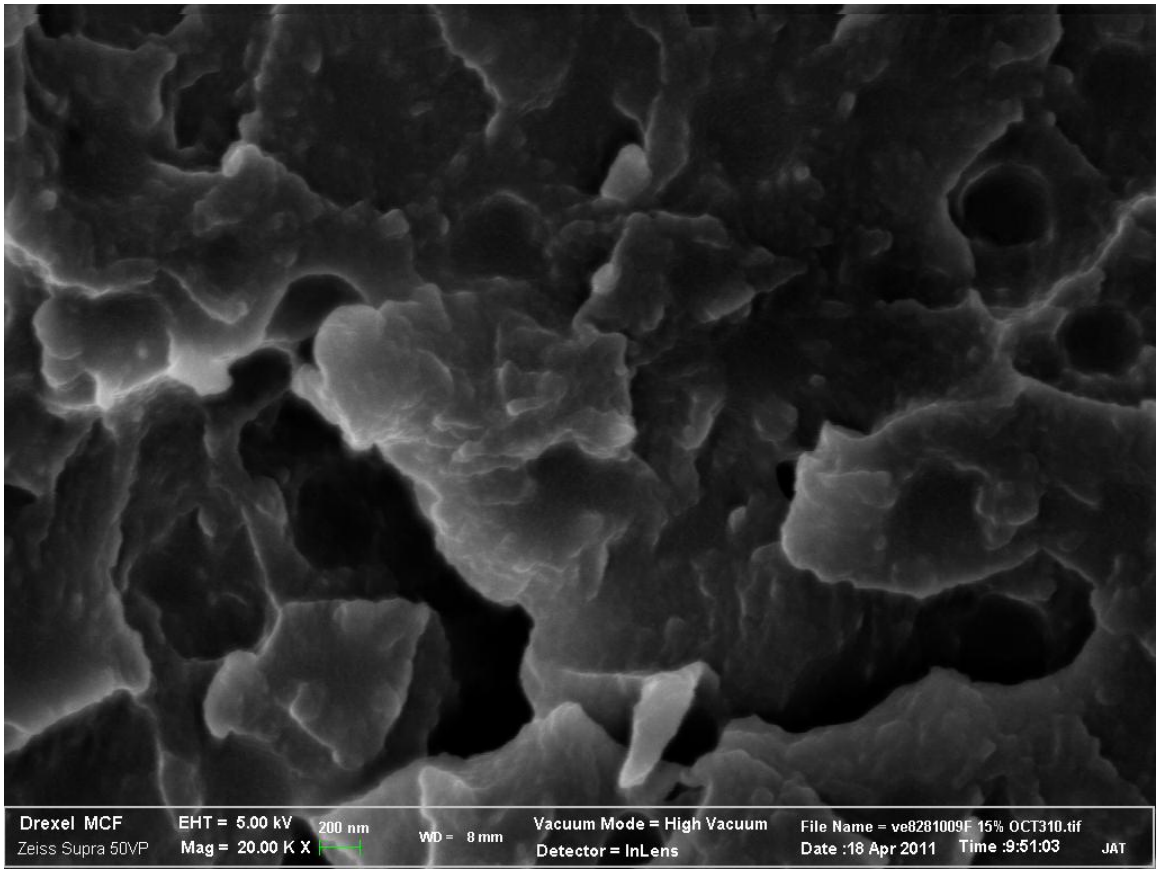

Figure 56: LN2 prepared VE 828-1009F 15% Oct 3.

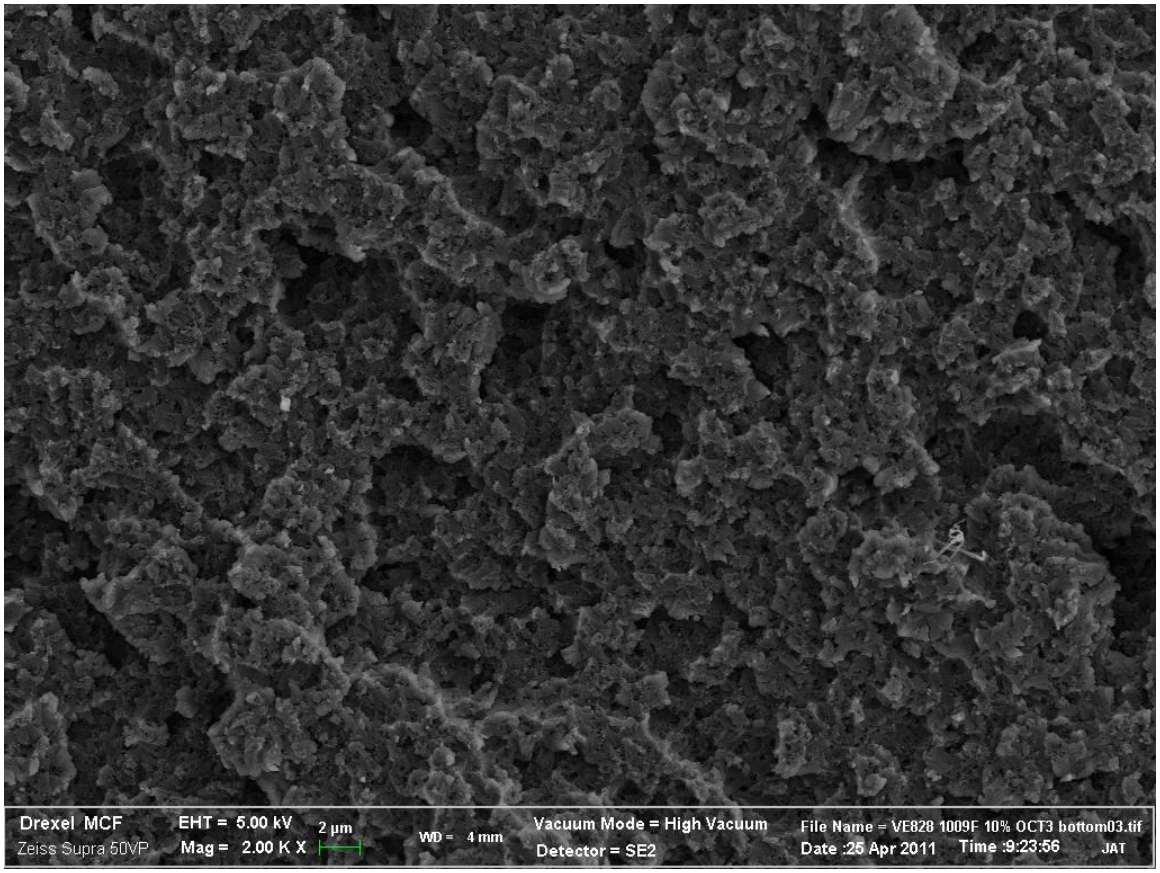

Figure 57: FT prepared VE 828-1009F 10% Oct 3.

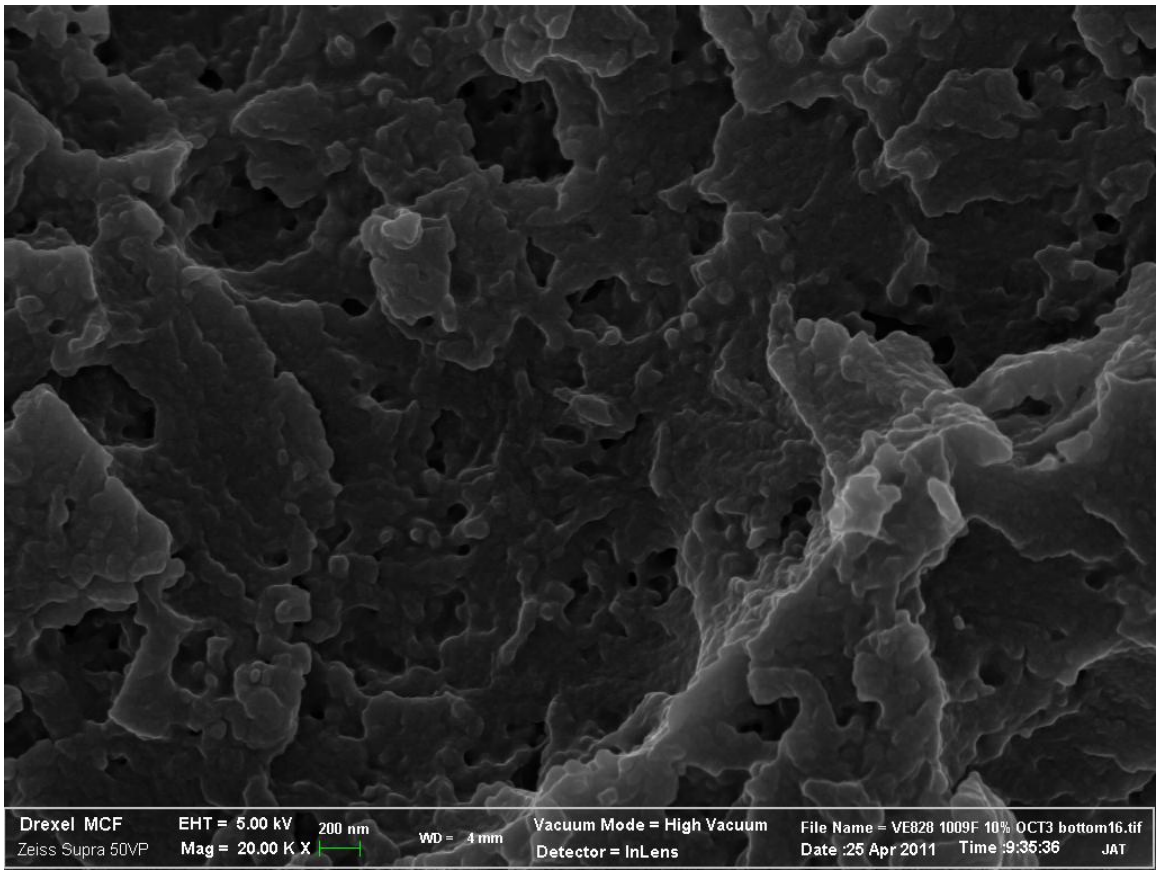

Figure 58: FT prepared VE 828-1009F 10% Oct 3.

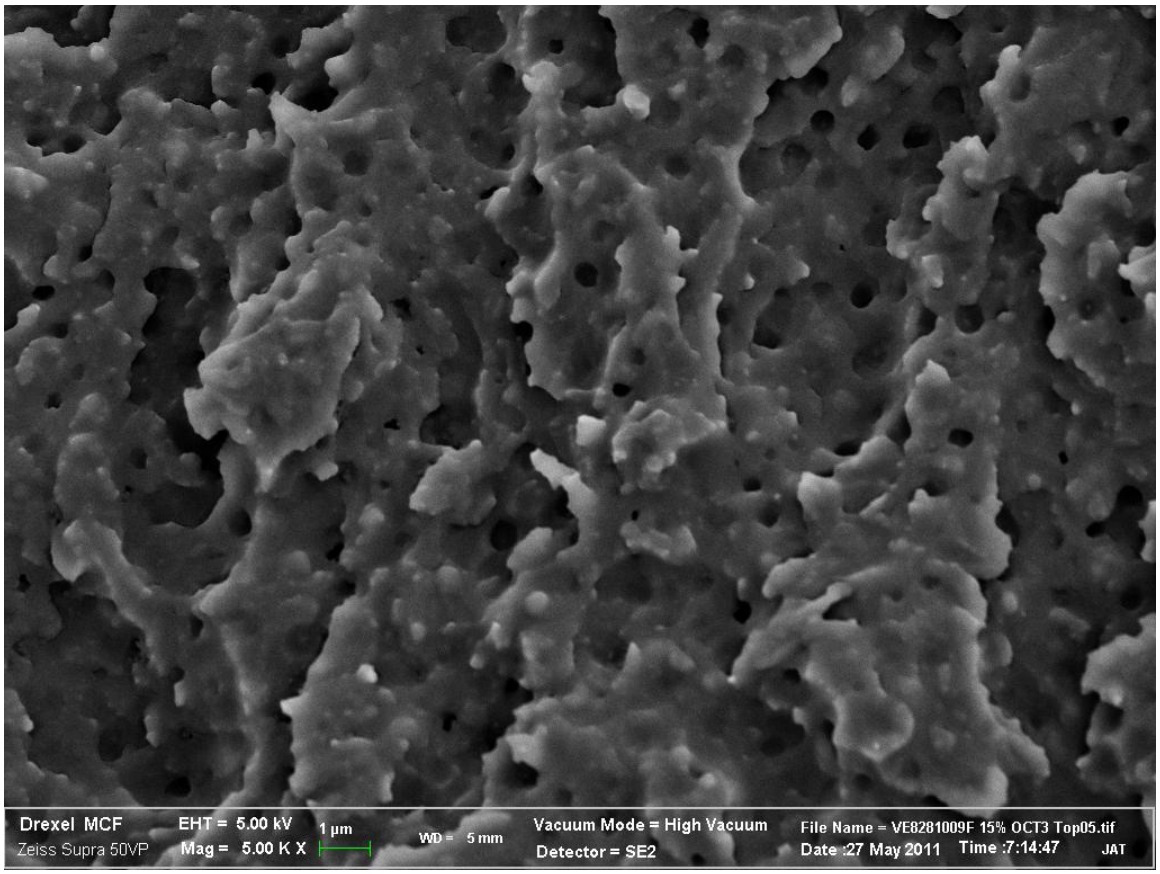

Figure 59: FT prepared VE 828-1009F 15% Oct 3.